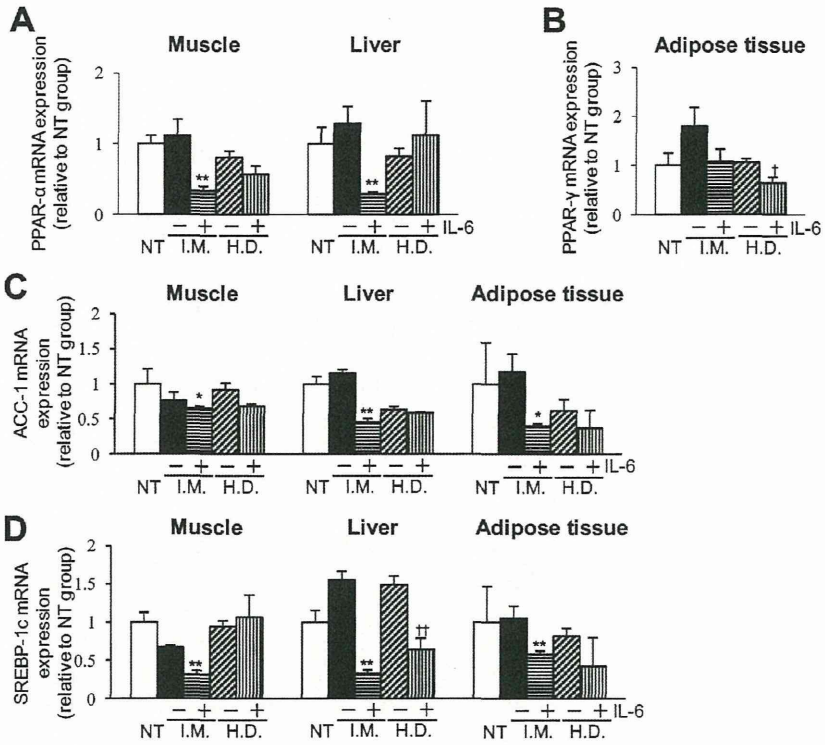

Figure 5. Effect of IL-6 gene delivery on the mRNA expression of lipid metabolism-related genes in the muscle, liver, and adipose tissue. DIO mice received an intramuscular injection (I.M.) of pcDNA3.1 (mock) (200 μg/mouse) or pCMV-IL-6 (200 μg/mouse) or a hydrodynamic injection (H.D.) of pCpG-mcs (mock) (0.75 μg/g bodyweight) or pGpG-IL-6 (0.75 μg/g bodyweight) and were sacrificed on day 14. (A) mRNA expression of PPAR-α in the muscle and liver. (B) mRNA expression of PPAR-γ in the adipose tissue. (C, D) mRNA expression of (C) ACC-1 and (D) SREBP-1c in the muscle, liver, and adipose tissue. The results are expressed as the mean + SE of five mice except for the H.D. injection in the pCpG-IL-6 group ($n = 3$). *$P < 0.05$ and **$P < 0.01$ compared with the mock intramuscular injection group. †$P < 0.05$ and ††$P < 0.01$ compared with the mock hydrodynamic injection group.

pDNA (Figure 3). However, the hydrodynamic injection of IL-6-expressing pDNA significantly reduced the mRNA expression level of PK1, G6Pase, and GYS in the liver (Figure 3C,F), but it did not significantly change the mRNA expression level of the other genes.

Effect of IL-6 Gene Transfer on the Obese State of DIO Mice. IL-6 gene delivery to the skeletal muscle and liver gradually reduced the body weight of DIO mice (Figure 4A). Gene transfer also reduced the food intake for the first week but only moderately reduced it for the second week (Figure 4B). To evaluate the changes in energy expenditure produced by IL-6 at the molecular level, we measured the mRNA expression level of UCP-2, a key enzyme involved in converting chemical energy into thermal energy. The UCP-2 mRNA expression level was significantly increased in the liver by IL-6 gene delivery (Figure 4C). The UCP-2 mRNA expression level in the muscle and adipose tissue was not significantly changed.

Next, we measured the serum concentrations of NEFA, TG, and cholesterol to evaluate further the lipid-metabolism status in DIO mice. The NEFA level was significantly reduced by IL-6 gene delivery (Figure 4D). The TG level was significantly reduced by the intramuscular gene delivery of IL-6 but not by hydrodynamic delivery (Figure 4E). The cholesterol level, however, was hardly changed by IL-6 gene delivery (Figure 4F).

We then measured the weight of the epididymal fat pad (Figure 4G). The fat pad weight of mice that received IL-6 gene delivery was moderately smaller than that of the corresponding control groups, although the difference was not significant. Examination of the HE-stained adipose tissue sections revealed that the adipocyte size was reduced by IL-6 gene delivery (Figure 4H–M). To evaluate quantitatively the size of the adipocytes, the number of adipocytes per field was counted (Figure 4N). The average size of the adipocytes in mice receiving IL-6 gene delivery was significantly smaller than in the mock-treated groups.

Effect of IL-6 Gene Delivery on the mRNA Expression of Lipid Metabolism-Related Genes in the Skeletal Muscle, Liver, and Adipose Tissue. To evaluate the effect of IL-6 gene delivery on lipid metabolism, the mRNA expression level of genes related to lipogenesis in the skeletal muscle, liver, and adipose tissue was measured (Figure 5). The function of ACC-1 is to provide the malonyl-CoA substrate for the biosynthesis of fatty acids, and SREBP-1 is a lipogenic transcription factor. IL-6 gene transfer showed a trend toward reduced mRNA expression of lipogenic genes compared with that in the mock-treated group. A greater reduction was observed in the mice that received an intramuscular injection of IL-6-expressing pDNA compared with those that received a hydrodynamic injection of IL-6-expressing pDNA.

Effect of IL-6 Gene Transfer on Inflammation. Next, we evaluated the inflammatory status after IL-6 gene delivery. To evaluate the degree of systemic inflammation induced by IL-6, the serum concentration of SAA, a representative pro-inflammatory protein, was measured on day 14. As shown in

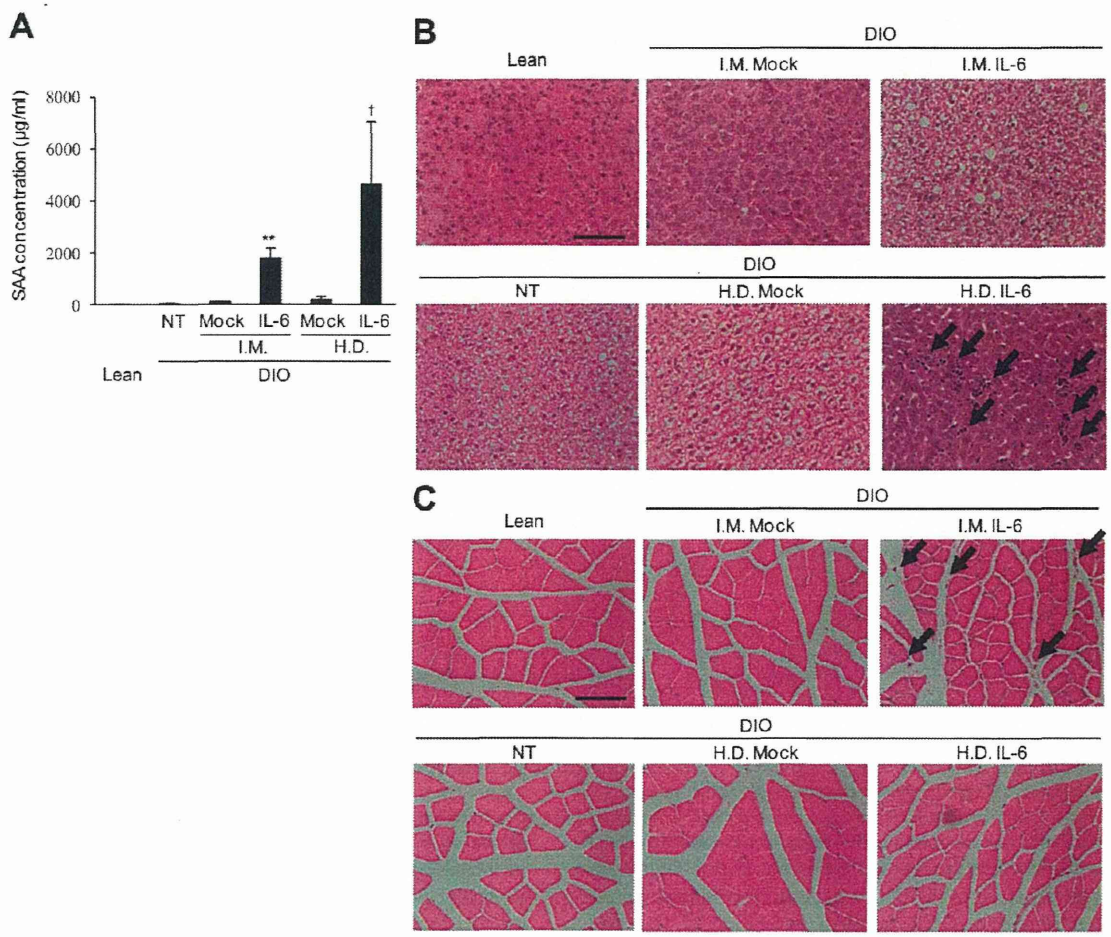

Figure 6. Effect of IL-6 gene delivery on inflammation. DIO mice received an intramuscular injection (I.M.) of pcDNA3.1 (mock) (200 μg/mouse) or pCMV-IL-6 (200 μg/mouse) or a hydrodynamic injection (H.D.) of pCpG-mcs (mock) (0.75 μg/g bodyweight) or pGpG-IL-6 (0.75 μg/g bodyweight). (A) SAA concentration in the serum on day 14. The results are expressed as the mean +SE of five mice except for the H.D. injection in the pCpG-IL-6 group (n = 3). $^{**}P < 0.01$ compared with the mock intramuscular injection group. $^{\dagger}P < 0.05$ compared with the mock hydrodynamic injection group. (B, C) Representative images of HE-stained (B) liver and (C) muscle sections. The arrows indicate the infiltration of inflammatory cells. The scale bar is 100 μm.

Figure 6A, serum levels of SAA were increased by IL-6 gene transfer.

The HE-stained liver sections revealed that there were a large number of glycogen vacuoles in the liver of the untreated DIO mice and mock-treated DIO mice (Figure 6B). In the liver sections of DIO mice that received a hydrodynamic injection of IL-6-expressing pDNA, an infiltration of inflammatory cells was observed. No infiltration of inflammatory cells was observed in the liver of DIO mice that received an intramuscular injection of IL-6-expressing pDNA. In the HE-stained muscle sections, an infiltration of inflammatory cells was observed in the injected muscle of the mice that were given IL-6-expressing pDNA by intramuscular injection (Figure 6C). No infiltration of inflammatory cells was observed in the muscle of the mice that received a hydrodynamic injection of IL-6-expressing pDNA.

Effect of Transient IL-6-Expression on GTT and Body Weight in DIO Mice. To confirm whether the sustained expression of IL-6 is required for the improvement of glucose homeostasis, DIO mice received a hydrodynamic injection of pCMV-IL-6 instead of pCpG-IL-6. In our previous studies, we demonstrated that hydrodynamic injection of the pCMV vector produces a transient transgene expression.[24] As expected, the mice showed a high IL-6 concentration on day 1 and then the concentration fell quickly (Figure 7A). The AUC and MRT values were 150 ± 60 ng/(mL·day) and 0.26 ± 0.02 days, respectively. On day 2, mice given pCMV-IL-6 showed similar glucose levels to those of the lean mice in the GTT (Figure 7B). On 7 and 14 days after pDNA administration, mice given pCMV-IL-6 showed higher glucose concentrations in the GTT (Figure 7B), although the glucose level was lower than the level before the administration of pCMV-IL-6. The changes in the body weight of the pCMV-IL-6-treated DIO mice were similar to those of the untreated DIO mice.

■ DISCUSSION

The involvement of IL-6 in glucose metabolism and insulin signaling has been suggested by previous studies. The present study has demonstrated that IL-6 exhibits positive effects on glucose metabolism in DIO mice after IL-6 gene transfer with both hydrodynamic delivery to the liver and intramuscular injection, corresponding well to the results obtained in most of

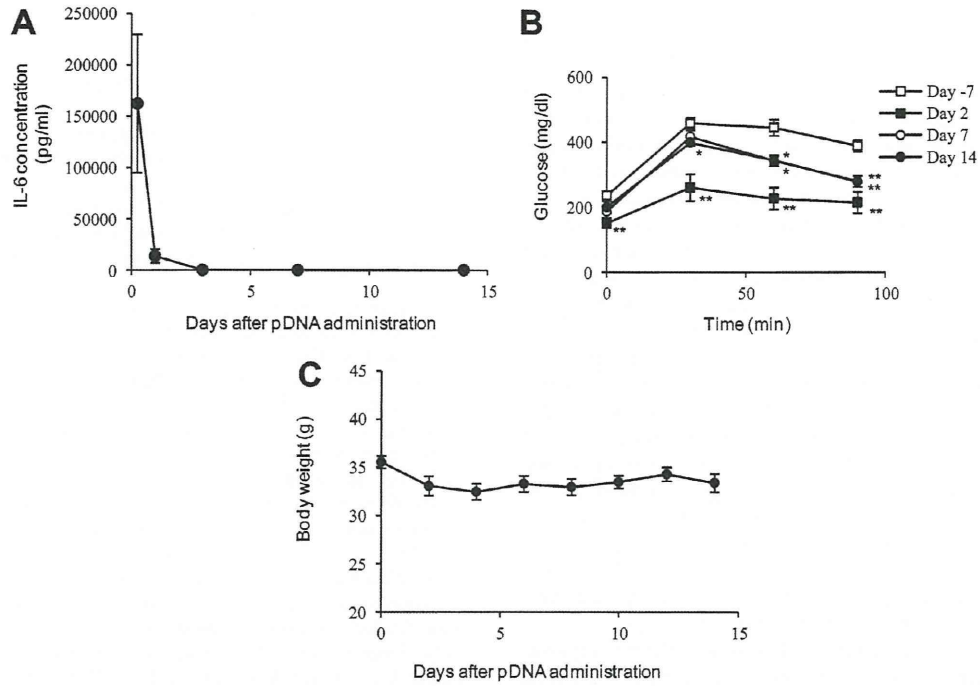

Figure 7. Effects of transient IL-6 expression on glucose homeostasis and obesity. DIO mice received a hydrodynamic injection of pCMV-IL-6 (0.25 μg/g bodyweight). (A) Time course of the concentration of IL-6 in the serum after gene delivery. (B) GTT test performed on days −7, 2, 7, and 14 after the hydrodynamic injection of pCMV-IL-6. The results are expressed as the mean ± SE of four mice.*$P < 0.05$ and **$P < 0.01$ compared with the day −7 group. (C) Body weight change after a 2-day interval.

the previous studies. Moreover, the pharmacokinetic profile of IL-6 has been shown to be an important factor. Significant effects were observed in the DIO mice that received a sustained IL-6 gene transfer, whereas transient expression of IL-6 had limited effects. The AUC value of each group was similar, whereas the MRT value in the mice with transient gene expression (0.26 ± 0.02 day) was significantly ($p < 0.01$) smaller than those (6.3 ± 0.4 and 3.8 ± 0.6 day) in the mice with sustained gene expression after intramuscular and hydrodynamic injection. These results suggest that a prolonged concentration in the circulation would be required for the positive pharmacodynamic actions of IL-6 in the DIO mice. With regard to the expression site of IL-6, the metabolic status, such as the mRNA expression level of metabolism-related genes and the serum insulin concentration, was improved more by the intramuscular injection than by the hydrodynamic injection. This observation suggests that the therapeutic effect of IL-6 in DIO mice is exerted via its action in the skeletal muscle rather than that in the liver, which is in agreement with previous studies.[14,20−22]

The decrease in body weight induced by IL-6 appears to be at least partly a result of the decrease in fat weight because we found that there was a reduction in the epididymal fat weight and adipocyte size (Figure 3). One possible reason for the fat reduction is the reduced food intake and increase in the expression level of energy-expenditure-related genes (Figure 4). Wallenius et al. showed that intracerebroventricular IL-6 treatment reduced body fat in DIO rats,[27] and this was caused by an increase in energy expenditure and a decrease in food intake. A study by Matthews et al. also demonstrated that genes associated with oxidative phosphorylation, the electron transport chain, and the tricarboxylic acid cycle were uniformly decreased in IL-6-deficient mice, which suggests that IL-6 has an increasing effect on energy expenditure.[28] Their results are consistent with our results that show that IL-6 gene delivery reduced food intake and increased energy expenditure, which implies that IL-6 expressed in the liver or skeletal muscle reached the brain and had an effect there. Moreover, the decrease in the mRNA expression level of lipid metabolism-related genes in the adipose tissue might be another reason for the reduction in the fat weight (Figure 5). We found that IL-6 gene delivery reduced the serum concentration of NEFA, which also suggests an improvement in the status of lipid metabolism by IL-6 gene delivery.

Regarding the relationship between the insulin sensitivity of muscle or liver and IL-6, some previous studies have reported that IL-6 enhanced insulin sensitivity in the muscle and increased insulin resistance in the liver.[20−22] The results of the current study showed that IL-6 gene delivery to both the liver and the muscle improved glucose metabolism (Figure 2). In addition, IL-6 gene delivery reduced the mRNA expression level of glucose metabolism-related genes in the liver and skeletal muscle (Figure 3). Moreover, IL-6 gene delivery reduced the serum insulin concentration in DIO mice (Figure 2). These results suggest that IL-6 gene delivery increased insulin sensitivity. Because SOCS-3 mRNA induction was observed in the muscle, liver, and adipose tissue after IL-6 gene delivery irrespective of the tissues transduced (Figure 1), IL-6 was expressed at the delivery site and transferred to distant tissues via the blood circulation. In fact, we observed high IL-6 concentrations in the blood circulation in both cases (Figure 1B). Recently, it was reported that IL-6 improved glycemia by stimulating glucagon-like peptide-1 (GLP-1) secretion from intestinal L cells and pancreatic alpha cells.[29] Therefore, IL-6 in

systemic circulation might stimulate GLP-1 secretion from those types of cells, although the GLP-1 concentration was not determined in the present study. The changes in insulin sensitivity on days 2 and 14 after the hydrodynamic injection of pCMV-IL-6 (Figure 7) indicate that the IL-6 concentration in the serum plays an important role in the overall improvement of insulin sensitivity after IL-6 gene delivery and that the IL-6-mediated improvement in insulin resistance is partially retained even after the level of IL-6 expression returned to normal.

In the present study, we have demonstrated that sustained supplementation of IL-6 improves the obese state and the metabolism of glucose and lipid in a mouse model of type II diabetes, suggesting that IL-6 gene delivery could be a therapeutic option for diabetes. However, great attention should be paid when using this approach because IL-6 is a typical inflammatory cytokine, which might cause serious side effects. In addition, long-term IL-6 therapy possesses a risk of inducing unexpected problems. In fact, a significant inflammation was observed in the site of IL-6 gene delivery in the present study, which is probably due to a high local concentration of IL-6. As chronic inflammation may accompany various types of diseases,[30] side effects including inflammation and inflammation-associated effects should be carefully monitored in performing IL-6 gene therapy.

We have demonstrated that IL-6 gene delivery improves systemic insulin sensitivity and obesity in a type II diabetes model. Our results clearly indicates that the time profile of IL-6 exposure is important for the effect of IL-6 in improving glucose and lipid metabolism.

AUTHOR INFORMATION

Corresponding Author

*Phone: +81-75-753-4580; Fax: +81-75-753-4614; E-mail: takakura@pharm.kyoto-u.ac.jp.

Author Contributions

The manuscript was written through contributions of all authors. All authors have given approval to the final version of the manuscript.

Notes

The authors declare no competing financial interest.

ACKNOWLEDGMENTS

This work was supported in part by a Grant-in-Aid for Scientific Research (B) from the Japan Society for the Promotion of Science (JSPS) and by a Grant-in-Aid for Scientific Research on hepatitis from the Japanese Ministry of Health, Labour, and Welfare of Japan.

REFERENCES

(1) Nathan, D. M.; Buse, J. B.; Davidson, M. B.; Ferrannini, E.; Holman, R. R.; Sherwin, R.; Zinman, B. Medical management of hyperglycaemia in type 2 diabetes mellitus: A consensus algorithm for the initiation and adjustment of therapy. A consensus statement from the American Diabetes Association and the European Association for the Study of Diabetes. *Diabetologia* **2009**, *52*, 17−30.

(2) Wagner, H.; Degerblad, M.; Thorell, A.; Nygren, J.; Ståhle, A.; Kuhl, J.; Brismar, T. B.; Öhrvik, J.; Efendic, S.; Båvenholm, P. N. Combined treatment with exercise training and acarbose improves metabolic control and cardiovascular risk factor profile in subjects with mild type 2 diabetes. *Diabetes Care* **2006**, *29*, 1471−1477.

(3) Tufescu, A.; Kanazawa, M.; Ishida, A.; Lu, H.; Sasaki, Y.; Ootaka, T.; Sato, T.; Kohzuki, M. Combination of exercise and losartan enhances renoprotective and peripheral effects in spontaneously type 2 diabetes mellitus rats with nephropathy. *J. Hypertens.* **2008**, *26*, 312−321.

(4) Febbraio, M. A.; Pedersen, B. K. Muscle-derived interleukin-6: Mechanisms for activation and possible biological roles. *FASEB J.* **2002**, *16*, 1335−1347.

(5) Pedersen, B. K.; Febbraio, M. A. Muscle as an endocrine organ: Focus on muscle-derived interleukin-6. *Physiol. Rev.* **2008**, *88*, 1379−1406.

(6) Helge, J. W.; Stallknecht, B.; Pedersen, B. K.; Galbo, H.; Kiens, B.; Richter, E. A. The effect of graded exercise of IL-6 release and glucose uptake in human skeletal muscle. *J. Physiol.* **2003**, *546*, 299−305.

(7) Carey, A. L.; Febbraio, M. A. Interleukin-6 and insulin sensitivity: Friend or foe? *Diabetologia* **2004**, *47*, 1135−1142.

(8) Glund, S.; Krook, A. Role of interleukin-6 signalling in glucose and lipid metabolism. *Acta Physiol.* **2008**, *192*, 37−48.

(9) Tsigos, C.; Papanicolaou, D. A.; Kyrou, I.; Defensor, R.; Mitsiadis, C. S.; Chrousos, G. P. Dose-dependent effects of recombinant human interleukin-6 on glucose regulation. *J. Clin. Endocrinol. Metab.* **1997**, *82*, 4167−4170.

(10) Fève, B.; Bastard, J. P. The role of interleukins in insulin resistance and type 2 diabetes mellitus. *Nat. Rev. Endocrinol.* **2009**, *5*, 305−311.

(11) Wallenius, V.; Wallenius, K.; Ahrén, B.; Rudling, M.; Carlsten, H.; Dickson, S. L.; Ohlsson, C.; Jansson, J. O. Interleukin-6-deficient mice develop mature-onset obesity. *Nat. Med.* **2002**, *8*, 75−79.

(12) Fosgerau, K.; Galle, P.; Hansen, T.; Albrechtsen, A.; De Lemos Rieper, C.; Pedersen, B. K.; Larsen, L. K.; Thomsen, A. R.; Pedersen, O.; Hansen, M. B.; Steensberg, A. Interleukin-6 autoantibodies are involved in the pathogenesis of a subset of type 2 diabetes. *J. Endocrinol.* **2010**, *204*, 265−273.

(13) Sadagurski, M.; Norquay, L.; Farhang, J.; D'Aquino, K.; Copps, K.; White, M. F. Human IL6 enhances leptin action in mice. *Diabetologia* **2010**, *53*, 525−535.

(14) Franckhauser, S.; Elias, I.; Rotter Sopasakis, V.; Ferré, T.; Nagaev, I.; Andersson, C. X.; Agudo, J.; Ruberte, J.; Bosch, F.; Smith, U. Overexpression of Il6 leads to hyperinsulinaemia, liver inflammation and reduced body weight in mice. *Diabetologia* **2008**, *51*, 1306−1316.

(15) Klover, P. J.; Zimmers, T. A.; Koniaris, L. G.; Mooney, R. A. Chronic exposure to interleukin-6 causes hepatic insulin resistance in mice. *Diabetes* **2003**, *52*, 2784−2789.

(16) Senn, J. J.; Klover, P. J.; Nowak, I. A.; Mooney, R. A. Interleukin-6 induces cellular insulin resistance in hepatocytes. *Diabetes* **2002**, *51*, 3391−3399.

(17) Senn, J. J.; Klover, P. J.; Nowak, I. A.; Zimmers, T. A.; Koniaris, L. G.; Furlanetto, R. W.; Mooney, R. A. Suppressor of cytokine signaling-3 (SOCS-3), a potential mediator of interleukin-6-dependent insulin resistance in hepatocytes. *J. Biol. Chem.* **2003**, *278*, 13740−13746.

(18) Inoue, H.; Ogawa, W.; Asakawa, A.; Okamoto, Y.; Nishizawa, A.; Matsumoto, M.; Teshigawara, K.; Matsuki, Y.; Watanabe, E.; Hiramatsu, R.; Notohara, K.; Katayose, K.; Okamura, H.; Kahn, C. R.; Noda, T.; Takeda, K.; Akira, S.; Inui, A.; Kasuga, M. Role of hepatic STAT3 in brain-insulin action on hepatic glucose production. *Cell Metab.* **2006**, *3*, 267−275.

(19) Weigert, C.; Hennige, A. M.; Lehmann, R.; Brodbeck, K.; Baumgartner, F.; Schaüble, M.; Häring, H. U.; Schleicher, E. D. Direct cross-talk of interleukin-6 and insulin signal transduction via insulin receptor substrate-1 in skeletal muscle cells. *J. Biol. Chem.* **2006**, *281*, 7060−7067.

(20) Nieto-Vazquez, I.; Fernandez-Veledo, S.; De Alvaro, C.; Lorenzo, M. Dual role of interleukin-6 in regulating insulin sensitivity in murine skeletal muscle. *Diabetes* **2008**, *57*, 3211−3221.

(21) Al-Khalili, L.; Bouzakri, K.; Glund, S.; Lönnqvist, F.; Koistinen, H. A.; Krook, A. Signaling specificity of interleukin-6 action on glucose and lipid metabolism in skeletal muscle. *Mol. Endocrinol.* **2006**, *20*, 3364−3375.

(22) Mennuni, C.; Calvaruso, F.; Zampaglione, I.; Rizzuto, G.; Rinaudo, D.; Dammassa, E.; Ciliberto, G.; Fattori, E.; La Monica, N. Hyaluronidase increases electrogene transfer efficiency in skeletal muscle. *Hum. Gene Ther.* **2002**, *13*, 355−365.
(23) Liu, F.; Song, Y. K.; Liu, D. Hydrodynamics-based transfection in animals by systemic administration of plasmid DNA. *Gene Ther.* **1999**, *6*, 1258−1266.
(24) Mitsui, M.; Nishikawa, M.; Zang, L.; Ando, M.; Hattori, K.; Takahashi, Y.; Watanabe, Y.; Takakura, Y. Effect of the content of unmethylated CpG dinucleotides in plasmid DNA on the sustainability of transgene expression. *J. Gene Med.* **2009**, *11*, 435−443.
(25) Hattori, K.; Nishikawa, M.; Watcharanurak, K.; Ikoma, A.; Kabashima, K.; Toyota, H.; Takahashi, Y.; Takahashi, R.; Watanabe, Y.; Takakura, Y. Sustained exogenous expression of therapeutic levels of IFN-γ ameliorates atopic dermatitis in NC/Nga mice via Th1 polarization. *J. Immunol.* **2010**, *184*, 2729−2735.
(26) Yamaoka, K.; Nakagawa, T.; Uno, T. Statistical moments in pharmacokinetics. *J. Pharmacokinet. Biopharm.* **1978**, *6*, 547−558.
(27) Wallenius, K.; Wallenius, V.; Sunter, D.; Dickson, S. L.; Jansson, J. O. Intracerebroventricular interleukin-6 treatment decreases body fat in rats. *Biochem. Biophys. Res. Commun.* **2002**, *293*, 560−565.
(28) Matthews, V. B.; Allen, T. L.; Risis, S.; Chan, M. H. S.; Henstridge, D. C.; Watson, N.; Zaffino, L. A.; Babb, J. R.; Boon, J.; Meikle, P. J.; Jowett, J. B.; Watt, M. J.; Jansson, J. O.; Bruce, C. R.; Febbraio, M. A. Interleukin-6-deficient mice develop hepatic inflammation and systemic insulin resistance. *Diabetologia* **2010**, *53*, 2431−2441.
(29) Ellingsgaard, H.; Hauselmann, I.; Schuler, B.; Habib, A. M.; Baggio, L. L.; Meier, D. T.; Eppler, E.; Bouzakri, K.; Wueest, S.; Muller, Y. D.; Hansen, A. M. K.; Reinecke, M.; Konrad, D.; Gassmann, M.; Reimann, F.; Halban, P. A.; Gromada, J.; Drucker, D. J.; Gribble, F. M.; Ehses, J. A.; Donath, M. Y. Interleukin-6 enhances insulin secretion by increasing glucagon-like peptide-1 secretion from L cells and alpha cells. *Nat. Med.* **2011**, *17*, 1481−1489.
(30) Straub, R. H. Evolutionary medicine and chronic inflammatory state–known and new concepts in pathophysiology. *J. Mol. Med.* **2012**, *90*, 523−534.

Gene Delivery of Albumin Binding Peptide-Interferon-gamma Fusion Protein with Improved Pharmacokinetic Properties and Sustained Biological Activity

NORIKO MIYAKAWA,[1] MAKIYA NISHIKAWA,[1] YUKI TAKAHASHI,[1] MITSURU ANDO,[1] MASAYUKI MISAKA,[1] YOSHIHIKO WATANABE,[2] YOSHINOBU TAKAKURA[1]

[1]Department of Biopharmaceutics and Drug Metabolism, Graduate School of Pharmaceutical Science, Kyoto University, Kyoto 606-8501, Japan

[2]Department of Molecular Microbiology, Graduate School of Pharmaceutical Science, Kyoto University, Kyoto 606-8501, Japan

Received 7 November 2012; revised 31 January 2013; accepted 12 February 2013

Published online 5 March 2013 in Wiley Online Library (wileyonlinelibrary.com). DOI 10.1002/jps.23493

ABSTRACT: We have demonstrated that gene delivery of a fusion protein of mouse interferon (IFN) γ with mouse serum albumin (IFNγ–MSA) was effective in prolonging the circulation half-life of IFNγ in mice. However, the fusion to MSA greatly reduced the biological activity of IFNγ to less than 1%. In this study, we designed IFNγ fusion proteins with a 20 amino-acid long albumin-binding peptide (ABP) to prolong the *in vivo* half-life of IFNγ without reducing its biological activity. IFNγ–ABP and ABP–IFNγ, two fusion proteins with the ABP being fused to the C- or N-terminal of IFNγ, retained 40%–50% biological activities determined using a gamma-activated sequence-dependent luciferase assay. These fusion proteins exhibited the ability to bind to MSA. Gene delivery of IFNγ–ABP or ABP–IFNγ to mice using the hydrodynamic injection method resulted in a sustained concentration of IFNγ in the serum compared with gene delivery of IFNγ. In addition, the growth of mouse colon carcinoma CT-26 cells in the lung was efficiently inhibited by gene delivery of the IFNγ fusion proteins. These results indicate that the fusion of ABP is a useful approach to achieving prolonged retention in the blood circulation through binding to serum albumin and retaining biological activity. © 2013 Wiley Periodicals, Inc. and the American Pharmacists Association J Pharm Sci 102:3110–3118, 2013

Keywords: albumin; albumin-binding peptide; biological activity; clearance; fusion protein; gene delivery; hydrodynamic injection; moment analysis; plasmid DNA; pharmacokinetics

INTRODUCTION

Interferon-gamma (IFNγ) is a pleiotropic cytokine with antiviral, antiproliferative, and immunomodulatory activities.[1,2] Despite extensive studies in the last two decades, the clinical application of IFNγ is limited to the treatment of a small number of diseases, including chronic granulomatous disease, osteopetrosis, and renal cancer, largely because of its short *in vivo* half-life.[2–4] Frequent injections are required to maintain effective concentrations, but the fluctuating blood concentration of IFNγ produced by frequent dosing leads to serious adverse toxic effects, including fever, fatigue, and neurotoxicity.[2,5,6]

Gene delivery of a therapeutic protein with unsatisfactory pharmacokinetic properties, such as a short *in vivo* half-life, is a promising approach to achieving sustained therapeutic effects with minimal toxicity. In previous studies, we showed that plasmid-based gene delivery of IFNγ is effective in inhibiting metastatic tumor growth and atopic dermatitis in mice.[7–10] These studies indicated the therapeutic potential of IFNγ gene transfer in several disease models. However, we also found that high doses of IFNγ-expressing plasmids, especially those expressing IFNγ for a long period, induced toxic effects. We hypothesized that controlling the tissue distribution of IFNγ expressed from plasmid vectors would be a promising method of reducing such toxic effects. On the basis of this hypothesis, we designed fusion proteins of IFNγ with mouse serum albumin (MSA) and constructed plasmids encoding the fusion protein,

Correspondence to: Makiya Nishikawa (Telephone: +81-75-753-4580; Fax: +81-75-753-4614; E-mail: makiya@pharm.kyoto-u.ac.jp)

Journal of Pharmaceutical Sciences, Vol. 102, 3110–3118 (2013)

IFNγ–MSA.[11] The fusion to MSA resulted in prolongation of the mean residence time of IFNγ after gene delivery. However, the fusion also greatly reduced the biological activity of IFNγ and the IFNγ–MSA exhibited only about 1/200th of the activity of IFNγ.

Marked reduction in the biological activity produced by the fusion of MSA would be due to steric hindrance of the IFNγ–IFNγ receptor interaction by MSA because MSA has a molecular weight of 67,000.[12] Dennis et al.[13–15] reported that the conjugation of a phage-derived 20 amino-acid long albumin-binding peptide (ABP) gave IgG fragments high affinity for serum albumin, leading to an increased *in vivo* circulation half-life.[13–15] The low-molecular weight of the ABP, as well as the noncovalent binding to serum albumin, could prevent it from reducing the biological activity of IFNγ.

Here, we designed fusion proteins of IFNγ with ABP to increase the half-life of IFNγ without any marked reduction in its biological activity. ABP was fused to either the N- or C-terminal end of IFNγ with a short linker peptide. We constructed plasmid vectors encoding these fusion proteins and examined their biological activity and binding to serum albumin, and their serum levels after gene transfer in mice. Then, the therapeutic effects of gene delivery of IFNγ fusion protein were examined in mice with pulmonary metastases of colon carcinoma cells.

MATERIALS AND METHODS

Cell Culture and Animals

An African green monkey kidney fibroblast cell line, COS-7, was obtained from American Type Culture Collection (Manassas, Virginia). A murine melanoma cell line, B16-BL6, was obtained from the Cancer Chemotherapy Center of the Japanese Foundation for Cancer Research (Tokyo, Japan). B16-BL6 and COS-7 cells were cultured in Dulbecco's modified Eagle's medium supplemented with 10% heat-inactivated fetal bovine serum and penicillin–streptomycin–L-glutamine at 37°C. CT-26 cells were cultured in RPMI1640 medium supplemented with 10% heat-inactivated fetal bovine serum and penicillin–streptomycin–L-glutamine at 37°C. Four-week-old male ICR mice and BALB/c mice, approximately 20 g in weight, were purchased from Japan SLC, Inc. (Shizuoka, Japan), and maintained on a standard food and water diet under conventional housing conditions. All animal experiments were approved by the Institutional Animal Experimentation Committee.

Plasmid DNA

pcDNA3.1 was purchased from Invitrogen (Carlsbad, California). phRL–thymidine kinase (TK), a renilla luciferase-expressing plasmid under the control of herpes simplex virus TK promoter, was purchased from Promega (Madison, Wisconsin). pGAS–Luc, a firefly luciferase-expressing plasmid under the control of gamma-activated sequence (GAS) promoter, has been described previously.[11,16] pCMV–IFNγ, an IFNγ-expressing plasmid under the control of cytomegalovirus (CMV) promoter, has also been described previously.[11] pCMV–IFNγ–ABP and pCMV–ABP–IFNγ, a plasmid encoding IFNγ–ABP (ABP was fused to the C-terminal of IFNγ) or ABP–IFNγ (ABP was fused to the N-terminal), respectively, were constructed by the following method. An IFNγ–ABP or ABP–IFNγ cDNA fragment was amplified by polymerase chain reaction (PCR) from pCMV–IFNγ using a primer with the addition of ABP sequences (GRLMEDICIPRWGCLWEDDF)[14] to the C- or N-terminal of IFNγ. Oligonucleotides encoding a 4 amino-acid (GGGS) linker were inserted between IFNγ cDNA and ABP sequences according to a previous report.[14,17] The fragment was then inserted into the BamHI/XbaI sites of pcDNA3.1. Each plasmid was amplified in *Escherichia coli* (DH5α, TOYOBO, Osaka, Japan) and purified using a JETSTAR plasmid purification kit (GENOMED, Löhne, Germany).

In Vitro Transfection

Cells were seeded on 10 cm dishes at a density of 1×10^6 cells/dish or 12-well culture plates at 1×10^5 cells/well and incubated overnight and the cells were transfected with the indicated plasmid using Lipofectamine2000 (Invitrogen) according to the manufacturer's instructions. In brief, 1 μg plasmid was mixed with 3 μL Lipofectamine2000 in Opti-MEM (Invitrogen) at a final concentration of 2 μg DNA/mL and the complex obtained was added to cells. The total amount of plasmid DNA used for transfection was 8 μg/dish for 10 cm dishes and 1 μg/well for 12-well culture plates, respectively.

Collection of Conditioned Medium

COS-7 cells seeded on 10-cm dishes were transfected with pCMV–IFNγ, pCMV–IFNγ–ABP, or pCMV–ABP–IFNγ as described above. Four hour after transfection, cells were washed with PBS and cultured with serum-free Opti-MEM medium for 48 h. Then, the culture medium was collected as conditioned medium.

Western Blotting

The conditioned medium of COS-7 cells transfected with pCMV–IFNγ, pCMV–IFNγ–ABP, or pCMV–ABP–IFNγ were collected as described above. The samples were reduced by the addition of dithiothreitol (0.1 M) and heat treatment at 95°C for 4 min to disrupt the disulfide bonds and to dissociate any homodimers that might be present. The samples were

then applied onto 12.5% polyacrylamide gel and were electrophoresed in the presence of sodium dodecyl sulfate (SDS) at the voltage of 200 V for 40 min. After SDS-polyacrylamide gel electrophoresis (PAGE), proteins resolved in the gel were electrophoretically transferred to a PVDF membrane using a wet blotting method in a buffer containing 25 mM Tris, 192 mM glycine, and 20% methanol at the voltage of 200 V for 45 min. After blocking with 5% skimmed milk, the membrane was probed with goat antimouse IFNγ polyclonal antibody (R&D System, Inc., minneapolis, minnesota) overnight at 4°C and then allowed to react with antigoat IgG antibody conjugated with horseradish peroxidase (Santa Cruz, Inc., Santa Cruz, California) for 1 h at room temperature. The bands were detected with LAS-3000 (Fuji Film, Tokyo, Japan).

Measurement of the Biological Activity of IFNγ, IFNγ–ABP, and ABP–IFNγ

B16-BL6 cells were cotransfected with pGAS–Luc (1.4 μg/mL) and phRL–TK (0.6 μg/mL). After a 4 h transfection, the culture medium was replaced with fresh serum-free Opti-MEM containing serial dilutions of the conditioned medium of COS-7 cells transfected with pCMV–IFNγ, pCMV–IFNγ–ABP, or pCMV–ABP–IFNγ. After a 24 h incubation, cells were lysed with a lysis buffer (0.1 M Tris, 0.05% Triton-X-100, 2 mM ethylenediaminetetraacetic acid, pH 7.8) and the lysates were mixed with reagents of the Dual-Luciferase Reporter Assay System (Promega). Then, firefly and renilla luciferase activity was measured in a luminometer (Lumat LB 9507; EG&G Bethhold, Bad Wildbad, Germany) and the ratio of firefly luciferase activity to renilla luciferase activity was calculated. Here, firefly luciferase activity was used as an indicator of IFNγ-driven transcription and renilla luciferase activity was used for normalization of the transfection efficiency and cell number.[18] The firefly/renilla ratio of the cells treated with indicated concentrations of IFNγ, IFNγ–ABP, or ABP–IFNγ was divided by the firefly/renilla ratio of the cells cultured without IFNγ, IFNγ–ABP, or ABP–IFNγ to give fold increase in GAS-dependent luciferase activity relative to those of the untreated group. Finally, the half maximum effective concentration (EC50) of IFNγ, IFNγ–ABP, and ABP–IFNγ was calculated. In a separate set of experiments, 100 pg/mL of IFNγ, IFNγ–ABP, or ABP–IFNγ was incubated with or without 0.25 mg/mL of MSA (Sigma; St. Louis, MO, USA) in Opti-MEM at 37°C for 1 h, and added to B16-BL6 cells transfected with pGAS–Luc and phRL-TK. Then, the fold increase in GAS-dependent luciferase activity relative to that of the untreated group was calculated as described above.

Measurement of the Binding Affinity of IFNγ, IFNγ–ABP, and ABP–IFNγ for MSA

Mouse serum albumin was immobilized onto 96-well plates at a concentration of 2 μg/mL overnight at 4°C. Wells were added with serially diluted supernatants of COS-7 cells transfected with pCMV–IFNγ, pCMV–IFNγ–ABP, or pCMV–ABP–IFNγ. After incubation for 2 h at room temperature, each well was washed with phosphate buffered saline-0.05% Tween 20 and proteins bound to MSA were detected by enzyme-linked immunosorbent assay (ELISA) using antimouse IFNγ antibody (eBioscoence, San Diego, California).[13,14]

In Vivo Gene Transfer

For gene transfer to mouse liver, mice received a hydrodynamic injection via the tail vein of plasmid DNA dissolved in 1.6 mL saline within 5 s.[19,20] The dose of plasmids was set at 0.2 pmol/mouse based on preliminary experiments. At predetermined periods, blood was collected from the tail vein and the blood samples were kept at 4°C for 2 h and centrifuged at 8000*g* for 20 min to obtain serum.

Measurement of mRNA Expression of IFNγ, IFNγ–ABP, and ABP–IFNγ in the Liver

Six hours after gene transfer, mice were sacrificed and total RNA was extracted from approximately 50 mg liver samples using Sepasol RNA I Super (Nacalai Tesque, Kyoto, Japan). After removal of contaminated DNA by DNase I (Takara Bio, Shiga, Japan), reverse transcription was performed using a ReverTra Ace qPCR RT kit (TOYOBO), followed by RNaseH treatment (Ribonuclease H; Takara Bio). For a quantitative analysis of mRNA expression, a real-time PCR was carried out with total cDNA using KAPA SYBR FAST ABI Prism 2× qPCR Master Mix (KAPA BIOSYSTEMS, Boston, Massachusetts). The oligonucleotide primers used for amplification were: *Ifnγ*-sense: 5′-CGGCACAGTCATTGAAAGCCTA-3′, *Ifnγ*-antisense: 5′-GTTGCTGATGGCCTGATTGTC-3′, and *β-actin*-sense: 5′-CATCCGTAAAGACCTCTATGC-3′, *β-actin*-antisense: 5′-ATGGAGCCACCGATCCACA-3. Amplified products were detected via intercalation of the fluorescent dye using a StepOnePlus Real Time PCR System (Applied Biosystems, Foster City, California). The mRNA expression of IFNγ was normalized using the mRNA level of β-actin.

Measurement of the Concentrations of IFNγ, IFNγ–ABP, and ABP–IFNγ

The concentrations of IFNγ, IFNγ–ABP, and ABP–IFNγ in the supernatant of COS-7 cells or mouse serum were determined by ELISA using a

commercial kit (Ready-SET-Go! MuIFN-γ ELISA; eBioscience).

Clearance of IFNγ, IFNγ–ABP, and ABP–IFNγ after Intravenous Injection into Mice

To obtain IFNγ, IFNγ–ABP, and ABP–IFNγ proteins, mice received a hydrodynamic injection of pCMV–IFNγ, pCMV–IFNγ–ABP, or pCMV–ABP–IFNγ as described above at a dose of 5 pmol/mouse. At 12 h after injection, blood was collected from the inferior vena cava and the serum was obtained in the same manner as described above. The serum samples containing IFNγ, IFNγ–ABP, or ABP–IFNγ were injected into different mice via the tail vein and blood was periodically sampled. The dose of each protein was set at 8.5 μg IFNγ/kg, and this was quantified by ELISA.[11]

Experimental Metastatic Pulmonary Tumor Model

CT-26 cells were trypsinized and suspended in Hanks' balanced salt solution (HBSS). Cell suspensions containing 1×10^5 CT-26 cells in 200 μL HBSS were injected into the tail vein of syngeneic BALB/c mice to establish an experimental metastatic pulmonary tumor model. Then, 3 days after inoculation of the CT-26 cells, each plasmid was injected into the tail vein by the hydrodynamic injection method at a dose of 0.7 pmol/mouse. At 14 days after inoculation, mice were sacrificed and the lungs were collected. The lungs were immersed in 100% methanol to make metastatic colonies more visible. Then, the number of metastatic colonies on the lung surface was counted by the naked eye.[11,21]

Pharmacokinetic Analysis

The peak plasma concentrations (C_{max}) and the time of maximum serum concentration (t_{max}) were obtained from actual data recorded after injection or gene transfer. The area under the serum concentration–time curve (AUC) and mean retention time (MRT) were calculated using a moment analysis method. These parameters were calculated for each animal by integration to infinite time.[22]

Data Analysis

Differences were statistically evaluated by Student's *t*-test, and the level of statistical significance was set at $p < 0.05$.

RESULTS

Expression of IFNγ–ABP and ABP–IFNγ in Cultured Cells

Figure 1a shows the Western blot analysis of the expression of IFNγ, IFNγ–ABP, and ABP–IFNγ in

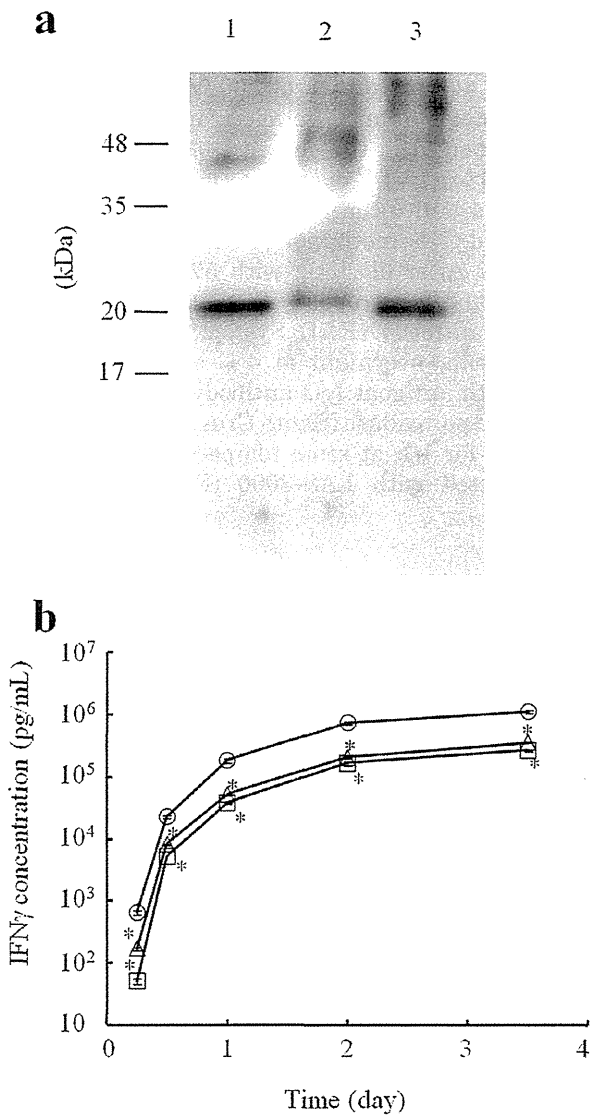

Figure 1. Expression of IFNγ–ABP and ABP–IFNγ in COS-7 cells. (a) Western blot analysis of IFNγ, IFNγ–ABP, and ABP–IFNγ. Western blotting was performed to confirm the molecular weight of IFNγ (lane 1), ABP–IFNγ (lane 2), and IFNγ–ABP (lane 3). Culture media of COS-7 cells transfected with pCMV–IFNγ, pCMV–ABP–IFNγ, and pCMV–IFNγ–ABP were subjected to 12.5% SDS-PAGE under reducing conditions. IFNγ, ABP–IFNγ, and IFNγ–ABP were detected with antimouse IFNγ polyclonal antibody. (b) Time course of the concentration of IFNγ (circles), IFNγ–ABP (squares), and ABP–IFNγ (triangles) in the culture medium of COS-7 cells after transfection of pCMV–IFNγ, pCMV–IFNγ–ABP, and pCMV–ABP–IFNγ (2 μg/mL). At the indicated time periods after transfection, the supernatants were collected and the concentration of IFNγ, ABP–IFNγ, or IFNγ–ABP was measured by ELISA using antimouse IFNγ antibody. The results are expressed as the mean ± standard error of the mean (SEM) of three independent determinations. $*p < 0.05$ compared with pCMV–IFNγ group.

COS-7 cells. Under reducing conditions, a band around 20 kDa was detected in the culture media of cells transfected with pCMV–IFNγ (lane 1), which is in good agreement with the size of monomeric IFNγ.[23] The supernatant of cells transfected with pCMV–IFNγ–ABP or pCMV–ABP–IFNγ also showed a band of slightly higher molecular mass of IFNγ (lanes 2 and 3, respectively), suggesting that the fusion proteins, IFNγ–ABP and ABP–IFNγ, were expressed from the plasmid vectors.

Figure 1b shows the time course of IFNγ, IFNγ–ABP, and ABP–IFNγ concentrations in culture media of COS-7 cells after transfection with pCMV–IFNγ, pCMV–IFNγ–ABP, or pCMV–ABP–IFNγ, respectively. The concentrations of IFNγ–ABP and ABP–IFNγ were significantly lower than that of IFNγ, although the shapes of the time courses were similar among all the groups.

Measurement of the Biological Activity of IFNγ–ABP and ABP–IFNγ

The biological activity of IFNγ–ABP and ABP–IFNγ was measured by GAS-dependent luciferase assay (Fig. 2a).[11,24,25] Addition of IFNγ to cells transfected with pGAS–Luc increased the luciferase activity of the cells in a concentration-dependent manner, confirming the validity of the method. IFNγ–ABP or ABP–IFNγ also dose-dependently increased the luciferase activity. The calculated EC50 values of IFNγ–ABP and ABP–IFNγ were 93 and 110 pg/mL, respectively, which indicates that IFNγ–ABP and ABP–IFNγ possess 46% and 40% of the activity of IFNγ (43 pg/mL). Thus, high biological activity remained after the fusion of ABP to IFNγ irrespective of the fusion sites. There was no significant difference in activity between IFNγ–ABP and ABP–IFNγ.

To investigate whether the biological activity of IFNγ, IFNγ–ABP, and ABP–IFNγ is affected by MSA, the GAS-dependent assay was carried out using IFNγ, IFNγ–ABP, or ABP–IFNγ incubated with or without 0.25 mg/mL of MSA (Fig. 2b). Presence of MSA hardly affected the activity of IFNγ, but it significantly reduced that of IFNγ–ABP and ABP–IFNγ.

Binding Affinity of IFNγ–ABP and ABP–IFNγ to Albumin

Figure 3 shows the amount of IFNγ, IFNγ–ABP, and ABP–IFNγ bound to MSA immobilized onto culture plates, determined using ELISA with anti-mouse IFNγ antibody. Both IFNγ–ABP and ABP–IFNγ bound to MSA in a dose-dependent manner. On the contrary, IFNγ hardly bound to MSA. The amount of ABP–IFNγ bound to MSA was significantly higher than that of IFNγ–ABP compared at the same concentrations, indicating the high affinity of the former. The fusion proteins showed much less binding to human serum albumin or bovine IgG (data not shown).

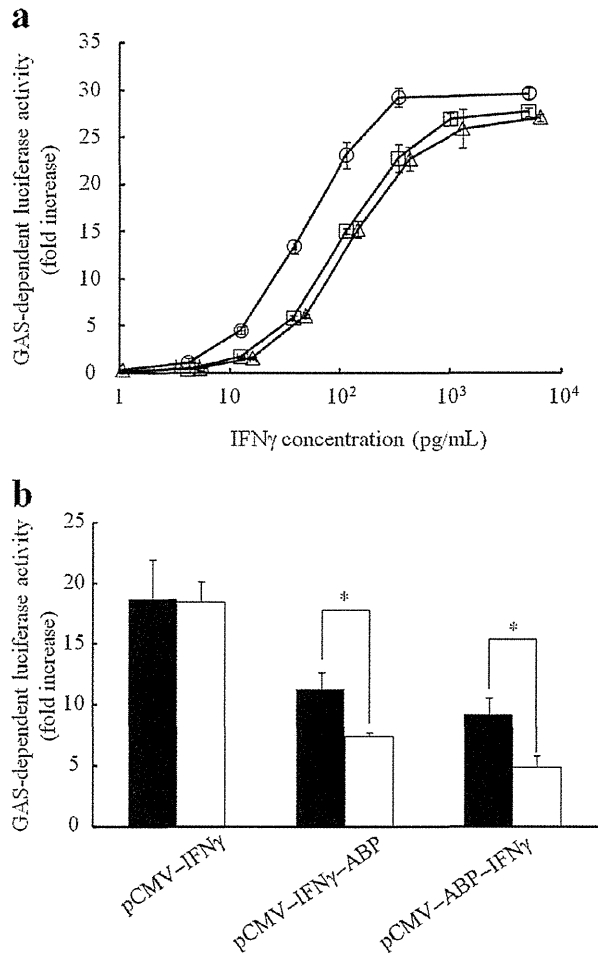

Figure 2. (a) Biological activity of IFNγ–ABP and ABP–IFNγ. B16–BL6 cells transfected with pGAS–Luc and phRL–TK were incubated with serial dilutions of IFNγ (circles), IFNγ–ABP (squares), or ABP–IFNγ (triangles) for a further 24 h. pGAS–Luc, plasmid DNA expressing firefly luciferase, was used to assess the degree of activation of the GAS signaling pathway. phRL–TK, plasmid DNA expressing renilla luciferase was used for normalization of the transfection efficiency and cell numbers. The ratio was normalized to give *x*-fold values relative to those of the untreated group and the half-maximum effective concentration (EC50) of IFNγ, IFNγ–ABP, and ABP–IFNγ was calculated. The results are expressed as the mean ± SEM of four independent determinations. (b) Biological activity of IFNγ, IFNγ–ABP, and ABP–IFNγ with or without MSA. IFNγ, IFNγ–ABP, and ABP–IFNγ (100 pg/mL) incubated with (open column) or without 0.25 mg/mL MSA (closed column) was added to B16–BL6 cells transfected with pGAS–Luc and phRL–TK. The results are expressed as the mean ± SEM of four independent determinations. $*p < 0.05$.

Clearance of IFNγ, IFNγ–ABP, and ABP–IFNγ after Intravenous Injection into Mice

To confirm whether the fusion of ABP increases the blood circulation time of IFNγ, IFNγ, IFNγ–ABP, and

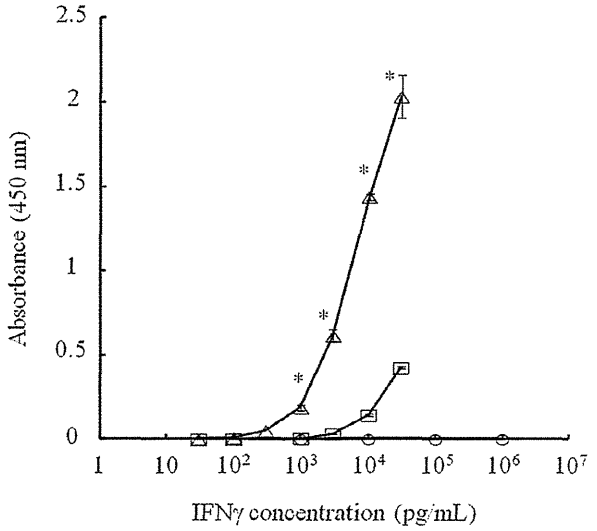

Figure 3. Binding of IFNγ–ABP and ABP–IFNγ to immobilized MSA. MSA was immobilized onto 96-well plates at a concentration of 2 μg/mL overnight. IFNγ (circles), IFNγ–ABP (squares), or ABP–IFNγ (triangles) was serially diluted and 100 μL amounts were added per well. After incubation for 2 h, bound proteins were detected by ELISA using antimouse IFNγ antibody. The results are expressed as the mean ± SEM of three independent determinations. $*p < 0.05$ compared with IFNγ–ABP group at the same concentration.

Table 1. Pharmacokinetic Parameters of IFNγ, IFNγ–ABP, and ABP–IFNγ after Intravenous Injection into Mice

Protein	IFNγ	IFNγ–ABP	ABP–IFNγ
AUC (ng h/mL)	57.6 ± 2.6	270 ± 24*	458 ± 5*
MRT (h)	2.64 ± 0.14	2.64 ± 0.07	4.11 ± 0.20*

The AUC and MRT were calculated by integration to infinite time, and the mean ± SEM values are shown.
*Statistically significant ($p < 0.05$) compared with IFNγ.

ABP–IFNγ were injected into the tail vein of mice. Figure 4 shows the time courses of the concentrations of IFNγ, IFNγ–ABP, and ABP–IFNγ in the serum after intravenous injection into mice at a dose of 8.5 μg IFNγ/kg body weight. The clearance of IFNγ–ABP and ABP–IFNγ was slower than that of IFNγ. The profiles were evaluated by moment analysis to calculate the AUC and MRT (Table 1). The AUC of IFNγ–ABP (270 ng h/mL) and ABP–IFNγ (458 ng h/mL) was significantly greater than that of IFNγ (57.6 ng h/mL). In addition, the MRT of ABP–IFNγ (4.11 h) was significantly longer than that of IFNγ (2.64 h) or IFNγ–ABP (2.69 h).

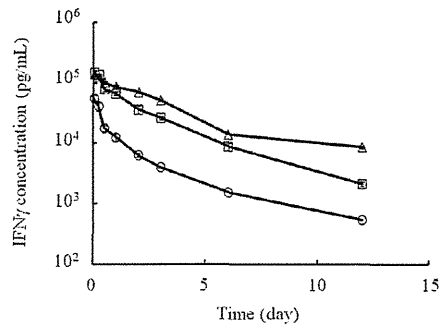

Figure 4. Clearance of IFNγ, IFNγ–ABP, and ABP–IFNγ after intravenous injection into mice. The concentrations of IFNγ (circles), IFNγ–ABP (squares), and ABP–IFNγ (triangles) were measured by ELISA using antimouse IFNγ antibody. The results are expressed as the mean ± SEM of four mice.

mRNA Expression of IFNγ, IFNγ-ABP, and ABP-IFNγ in the Liver and Time Course of the Serum Concentration of IFNγ, IFNγγABP, and ABP-IFN? after In Vivo Gene Transfer

Figure 5a shows the mRNA expression of IFNγ, IFNγ–ABP, and ABP–IFNγ in the liver at 6 h after hydrodynamic injection of pCMV–IFNγ, pCMV–IFNγ–ABP, or pCMV–ABP–IFNγ, respectively. The expression of IFNγ, IFNγ–ABP, and ABP–IFNγ was not significantly different from one another. Figure 5b shows the time courses of the serum concentrations of IFNγ, IFNγ–ABP, and ABP–IFNγ after hydrodynamic injection of pCMV–IFNγ, pCMV–IFNγ–ABP, or pCMV–ABP–IFNγ, respectively, at a dose of 0.2 pmol/mouse. The disappearance of IFNγ–ABP and ABP–IFNγ from the circulation was much slower than that of IFNγ. The C_{max} of IFNγ–ABP (516 ng/mL) and ABP–IFNγ (1940 ng/mL) was markedly greater than that of IFNγ (46.6 ng/mL). The time to reach the maximum serum concentration (t_{max}) of the fusion proteins was 0.5 (IFNγ–ABP) and 1 (ABP–IFNγ) day, which was later than that of IFNγ (0.25 day). Table 2 summarizes the AUC and MRT values after hydrodynamic injection of pCMV–IFNγ, pCMV–IFNγ–ABP, and pCMV–ABP–IFNγ. A hydrodynamic injection of pCMV–IFNγ–ABP or pCMV–ABP–IFNγ produced about a 25- or 140-fold greater AUC and a 1.5- or twofold longer MRT than seen with pCMV–IFNγ.

Inhibition of the Growth of Metastatic Pulmonary Tumor by Gene Transfer of IFNγ, IFNγ–ABP, or ABP–IFNγ in Mice

Figure 6 shows the number of metastatic colonies of CT-26 cells on the lung surface at 14 days after inoculation of CT-26 cells into the tail vein of mice. A hydrodynamic injection of pCMV–IFNγ, pCMV–IFNγ–ABP, or pCMV–ABP–IFNγ signifi-

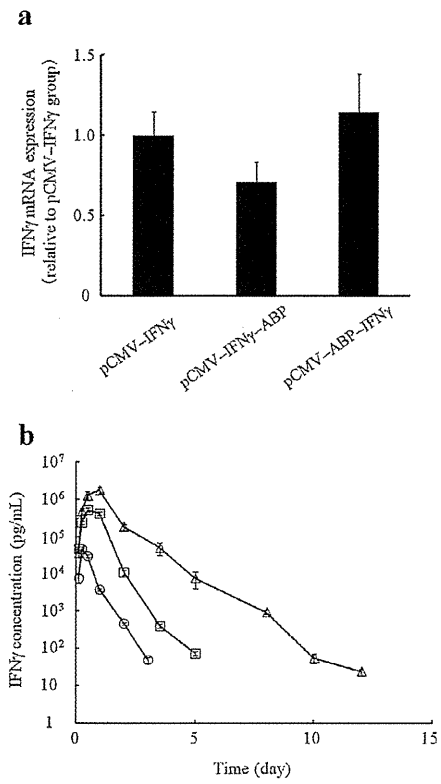

Figure 5. (a) mRNA expression of IFNγ, IFNγ–ABP, and ABP–IFNγ in the liver. mRNA expression of IFNγ, IFNγ–ABP, and ABP–IFNγ in the liver was measured 6 h after hydrodynamic injection of pCMV–IFNγ, pCMV–IFNγ–ABP, or pCMV–ABP–IFNγ into mice. The results are expressed as the mean ± SEM of three mice. (b) Time courses of the concentrations of IFNγ, IFNγ–ABP, and ABP–IFNγ in the serum after hydrodynamic injection of pCMV–IFNγ, pCMV–IFNγ–ABP, or pCMV–ABP–IFNγ into mice. Each plasmid DNA was administered at a dose of 0.2 pmol/mouse. The concentrations of IFNγ (circles), IFNγ–ABP (squares), andABP–IFNγ (triangles) were measured by ELISA using antimouse IFNγ antibody. The results are expressed as the mean ± SEM of three mice.

Table 2. Pharmacokinetic Parameters of IFNγ, IFNγ–ABP, and ABP–IFNγ after Hydrodynamic Injection of pCMV–IFNγ, pCMV–IFNγ–ABP, and pCMV–ABP–IFNγ, Respectively, into Mice

	IFNγ	IFNγ–ABP	ABP–IFNγ
AUC (ng h/mL)	24.3 ± 2.6	569 ± 58*	3430 ± 430*
MRT (h)	0.49 ± 0.01	0.79 ± 0.01*	1.03 ± 0.02*
C_{max} (ng/mL)	46.6 ± 3.2	516 ± 60*	1940 ± 240*
t_{max} (h)	6	12	24

The C_{max} and t_{max} values were obtained from actual data recorded after hydrodynamic injection of pCMV–IFNγ, pCMV–IFNγ–ABP, and pCMV–ABP–IFNγ at a dose of 0.2 pmol/mouse. The AUC and MRT were calculated by integration to infinite time, and the mean ± SEM values are shown.

*Statistically significant ($p < 0.05$) compared with pCMV–INFγ.

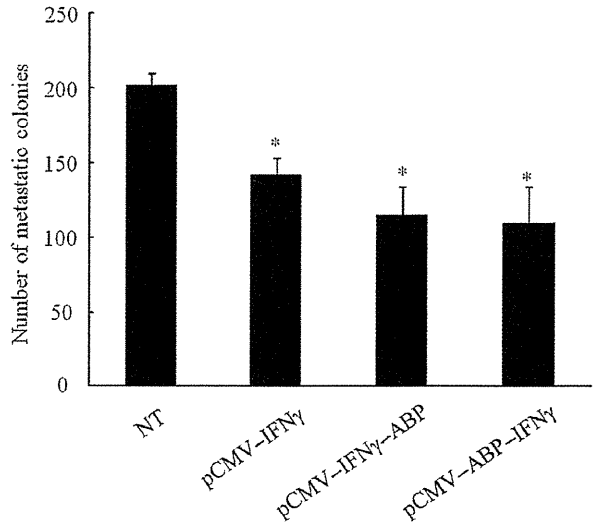

Figure 6. Number of metastatic colonies of CT-26 cells on the lung surface of mice. Pulmonary metastasis was induced by inoculation of 1×10^5 CT-26 cells into a tail vein (day 0). On day 3, pCMV–IFNγ, pCMV–IFNγ–ABP, or pCMV–ABP–IFNγ was injected into mice by hydrodynamic injection at a dose of 0.7 pmol/mouse. A group of control mice was left untreated (NT). At 14 days after tumor inoculation, mice were sacrificed and the number of metastatic colonies on the lung surface was counted. The results are expressed as the mean ± SEM of five mice. $*p < 0.05$ compared with the NT group.

cantly reduced the number of colonies to 70%, 56%, or 53% that in the no treatment group, respectively. There was no significant difference in the number of metastatic colonies among the groups.

DISCUSSION

Our previous study showed that the fusion of MSA to IFNγ dramatically improved the pharmacokinetic properties of IFNγ. However, the fusion also greatly reduced the biological activity of IFNγ.[11] Such reduction in the activity is similar to that of polyethylene glycol-conjugated human IFNα products used in clinical settings.[26] These results suggest that the use of serum albumin or other macromolecules is not suitable for the control of the pharmacokinetics of IFNγ. The present study clearly demonstrates that the fusion of a much smaller peptide (20 amino acids) than MSA is useful for controlling the tissue distribution of IFNγ without significantly reducing its biological activity.

Both IFNγ–ABP and ABP–IFNγ exhibited about 50% the activity of IFNγ, suggesting that the site of the fusion of ABP is of little importance. In addition, the reduced activity of IFNγ–ABP and ABP–IFNγ

in the presence of MSA (Fig. 2b) strongly suggests that the binding of IFNγ–ABP and ABP–IFNγ with MSA somewhat interferes with the binding of these fusion proteins to IFNγ receptor. It has been reported that both the N- and C-terminals of IFNγ are critical for the receptor interaction.[27,28] Because bioactive IFNγ is an antiparallel dimer,[1,29] fusion at either end would have a similar impact on the physiochemical properties of IFNγ. On the contrary, ABP–IFNγ exhibited higher binding affinity to MSA than IFNγ–ABP (Fig. 3), indicating that the fusion site did affect the interaction with MSA. A crystal structure analysis of human IFNγ revealed that both the N- and C-terminals are located on the surface of the molecule and the N-terminal is more flexible than the C-terminal which has some adjacent side chains.[30,31] Although there is little information on the structural properties of mouse INFγ, the helix of IFNγ is strongly conserved between mice and humans.[30,32] Therefore, the stronger binding activity of ABP–IFNγ to MSA, compared with IFNγ–ABP, is probably due to the greater flexibility of the N-terminal domain compared with the C-terminal.

Reflecting the binding to MSA, the fusion of ABP could prolong the circulation time of IFNγ. Similar results were observed after gene delivery of these derivatives. An injection of pCMV–ABP–IFNγ produced a higher AUC and longer MRT than that of pCMV–IFNγ–ABP (Table 2). These differences would be due to the difference in the binding affinity to MSA between these fusion proteins, as was the case with the protein injection, because the mRNA expression of IFNγ in the liver was comparable among all the groups (Fig. 5a). Taken together, these results clearly show that the gene delivery of IFNγ–ABP or ABP–IFNγ is an effective approach to improving the pharmacokinetic properties of IFNγ.

Effective inhibition of metastatic tumor growth by gene delivery of IFNγ–ABP or ABP–IFNγ indicates that these fusion proteins are pharmacologically active and their gene delivery is a promising therapeutic method for the treatment of a number of diseases. Although the affinity of IFNγ–ABP for MSA was higher than that of ABP–IFNγ, and no significant difference was observed in the number of metastatic colonies. A possible explanation of this is that the high affinity of the fusion protein for MSA disturbs its binding to the IFNγ receptor, as observed in the in vitro experiment (Fig. 2b). The results of the present study indicate that selecting or designing ABP with proper affinity for serum albumin can maximize the therapeutic effects of IFNγ by achieving optimal balance between biological activity and retention in blood circulation.

CONCLUSION

We have demonstrated that the fusion of ABP to IFNγ is a useful approach to achieving prolonged retention in blood circulation through binding to serum albumin and this prolonged retention is effective in inhibiting metastatic tumor growth in mouse lung.

ACKNOWLEDGMENTS

This work was supported in part by a Grant-in-Aid for Scientific Research (B) from the Japan Society for the Promotion of Science, and by a Grant-in-Aid for Research on Hepatitis from the ministry of Health, Labour, and Welfare of Japan.

REFERENCES

1. Farrar MA, Schreiber RD. 1993. The molecular cell biology of interferon-γ and its receptor. Annu Rev Immunol 11:571–611.
2. Jonasch E, Haluska FG. 2001. Interferon in oncological practice: Review of interferon biology, clinical applications, and toxicities. Oncologist 6:34–55.
3. Younes HM, Amsdem BG. 2002. Interferon-γ therapy: Evaluation of routes of administration and delivery systems. J Pharm Sci 91:2–17.
4. Miller CH, Maher SG, Young HA. 2009. Clinical use of interferon-γ. Ann N Y Acad Sci 1182:69–79.
5. Kurzrock R, Rosenblum MG, Sherwin SA, Rios A, Talpaz M, Quesada JR, Gutterman JU. 1985. Pharmacokinetics, single-dose tolerance, and biological activity of recombinant gamma-interferon in cancer patients. Cancer Res 45:2866–2872.
6. Ferenci P, Brunner H, Nachbaur K, Datz C, Gschwantler M, Hofer H, Stauber R, Hackl F, Jessner W, Rosenbeiger M, Steindl PM, Hegenbarth K, Gangl A, Vogel W. 2001. Combination of interferon induction therapy and ribavirin in chronic hepatitis C. Hepatology 34:1006–1011.
7. Kobayashi N, Kuramoto T, Chen S, Watanabe Y, Takakura Y. 2002. Therapeutic effect of intravenous interferon gene delivery with nacked plasmid DNA in murine metastasis model. Mol Ther 6:737–744.
8. Kawano H, Nishikawa M, Mitsui M, Takahashi Y, Kako K, Yamaoka K, Watanabe Y, Takakura Y. 2007. Improved anti-cancer effect of interferon gene transfer by sustained expression using CpG-reduced plasmid DNA. Int J Cancer 121:401–406.
9. Hattori K, Nishikawa M, Watcharanurak K, Ikoma A, Kabashima K, Toyota H, Takahashi Y, Takahashi R, Watanabe Y, Takakura Y. 2010. Sustained exogenous expression of therapeutic levels of IFN-γ ameliorates atopic dermatitis in NC/Nga mice via Th1 polarization. J Immunol 184:2729–2735.
10. Watcharanurak K, Nishikawa M, Takahashi Y, Kabashima K, Takahashi R, Takakura Y. 2013. Regulation of immunological balance by sustained interferon-γ gene transfer for acute phase of atopic dermatitis in mice. Gene Ther [Epub ahead of print.]
11. Miyakawa N, Nishikawa M, Takahashi Y, Ando M, Misaka M, Watanabe Y, Takakura Y. 2011. Prolonged circulation half-life of interferon γ activity by gene delivery of interferon γ-serum albumin fusion protein in mice. J Pharm Sci 100:2350–2357.
12. Subramanian GM, Fiscella M, Smith AL, Zeuzem S, McHutchison JG. 2007. Albinterferon α-2b: a genetic fusion protein for the treatment of chronic hepatitis C. Nat Biotechnol 25:1411–1419.
13. Dennis MS, Zhang M, Meng YG, Kadkhodayan M, Kirchhofer D, Combs D, Damico LA. 2002. Albumin binding as a general strategy for improving the pharmacokinetics of proteins. J Biol Chem 277:35035–35043.

14. Nguyen A, Reyes AE II, Zhang M, McDonald P, Wong WL, Damico LA, Dennis MS. 2005. The pharmacokinetics of an albumin-binding Fab (AB.Fab) can be modulated as a function of affinity for albumin. Protein Eng Des Sel 19:291–297.
15. Dennis MS, Jin H, Dugger D, Yang R, McFarland L, Ogasawara A, Williams C, Cole MJ, Ross S, Schwall R. 2005. Imaging tumors with an albumin-binding Fab, a novel tumor-targeting agent. Clin Cancer Res 11:7109–7121.
16. Kanno Y, Kozak CA, Schindler C, Driggers PH, Ennist DL, Gleason SL, Darnell JE Jr, Ozato K. 1993. The genomic structure of the murine ICSBP gene reveals the presence of the gamma interferon-responsive element, to which an ISGF3 α subunit (or similar) molecule binds. Mol Cell Biol 13:3951–3963.
17. Zhao HL, Yao XQ, Xue C, Wang Y, Xiong XH, Liu ZM. 2008. Increasing the homogeneity, stability and activity of human serum albumin and interferon-α2b fusion protein by linker engineering. Protein Expr Purif 61:73–77.
18. Takahashi Y, Kaneda H, Takasuka N, Hattori K, Nishikawa M, Takakura Y. 2008. Enhancement of antiproliferative activity of interferons by RNA interference-mediated silencing of SOCS gene expression in tumor cells. Cancer Sci 99:1650–1655.
19. Liu F, Song YK, Liu D. 1999. Hydrodynamics-based transfection in animals by systemic administration of plasmid DNA. Gene Ther 6:1258–1266.
20. Zhang GF, Budker V, Wolff JA. 1999. High levels of foreign gene expression in hepatocytes after tail vein injections of nacked plasmid DNA. Hum Gene Ther 10:1735–1737.
21. Mitsui M, Nishikawa M, Zang L, Ando M, Hattori K, Takahashi Y, Watanabe Y, Takakura Y. 2009. Effect of the content of unmethylated CpG dinucleotides in plasmid DNA on the sustainability of transgene expression. J Gene Med 11:435–443.
22. Yamaoka K, Nakagawa T, Uno T. 1978. Statistical moments in pharmacokinetics. J Pharmacokinet Biopharm 6:547–558.
23. Gribaudo G, Cofano F, Prat M, Baiocchi C, Cavallo G, Landolfo S. 1985. Natural murine interferon-γ. J Biol Chem 260:9936–9940.
24. Schroder K, Hertzog PJ, Ravasi T, Hume DA. 2004. Interferon-γ: An overview of signals, mechanisms and functions. J Leukoc Biol 75:163–189.
25. Stark GR, Kerr IM, Wiliams BR, Silverman RH, Schreiber RD. 1998. How cells respond to interferons. Annu Rev Biochem 67:227–264.
26. Veronese FM, Pasut G. 2005. Pegylation, successful approach to drug delivery. Drug Discov Today 10:1451–1458.
27. Griggs ND, Jarpe MA, Pace JL, Russell SW, Johnson HM. 1992. The N-terminus and C-terminus of IFN-γ are binding domains for cloned soluble IFN-γ receptor. J Immunol 149:517–520.
28. Lundell DJ, Narula SK. 1994. Structural elements required for receptor recognition of human interferon-γ. Pharmacol Ther 64:1–21.
29. Fountoulakis M, Juranville JF, Maris A, Ozmen L, Garotta G. One interferon γ receptor binds one interferon γ dimer. 1990. J Biol Chem 299:169–179.
30. Ealick SE, Cook WJ, Vijay-Kumar S, Carson M, Nagabhushan TL, Trotta PP, Bugg CE. 1991. Three-dimensional structure of recombinant human interferon-γ. Science 252:698–702.
31. Walter MR, Windsor WT, Nagabhushan TL, Lundell DJ, Lunn CA, Zauodny PJ, Narula SK. 2002. Crystal structure of a complex between interferon-γ and its soluble high-affinity receptor. Nature 376:230–235.
32. Savan R, Ravichandran S, Collins JR, Sakai M, Young HA. 2009. Structural conservation of interferon γ among vertebrates. Cytokine Growth Factor Rev 20:115–124.

Journal of Drug Targeting, 2012; 20(9): 764–769

ISSN 1061-186X print/ISSN 1029-2330 online
DOI: 10.3109/1061186X.2012.716848

informa
healthcare

REVIEW ARTICLE

Controlling the kinetics of interferon transgene expression for improved gene therapy

Kanitta Watcharanurak, Makiya Nishikawa, Yuki Takahashi, and Yoshinobu Takakura

Department of Biopharmaceutics and Drug Metabolism, Graduate School of Pharmaceutical Sciences, Kyoto University, Kyoto, Japan

Abstract

Interferon (IFN) gene based therapy has been studied for the treatment of many diseases such as viral infections, cancer and allergic diseases. Non-viral vectors, like plasmid DNA, are promising ways for delivering IFN genes, because of their low immunogenicity and toxicity compared with viral vectors. Potent therapeutic effects of IFN gene transfer will depend on the level and duration of transgene expression after *in vivo* administration. Therefore, controlling the kinetics of transgene expression of IFNs is a rational approach for improved gene therapy. The design and optimization of plasmid vectors, as well as their route/method of administration, is the key to obtaining high and persistent transgene expression. In this review, we aim to present experimental evidence about the relationships among the properties of plasmid vectors expressing IFNs, the kinetics of transgene expression, and therapeutic effects as well as safety issues.

Keywords: Non-viral vector, plasmid DNA, CpG motifs, plasmid backbone, promoter, enhancer

Introduction

Interferon (IFN) belongs to a family of cytokines, classified into three types based on the receptors with which they interact to initiate signal transduction. Type I IFN consists of many IFN subtypes including IFN-α and IFN-β. Type I IFNs signal through an IFN-α receptor complex. IFN-γ is the only IFN designated as a Type II IFN. IFN-γ binds to an IFN-γ receptor complex. The last and newest subgroup of IFNs, type III IFN, is IFN-λ. IFN-λ signals through a receptor complex consisting of IFN-λ receptor 1 and Interleukin-10 receptor 2. All types of IFNs have been shown to exert immunomodulatory, antiviral and antiproliferative effects. IFNs have been extensively studied as a treatment for many diseases, such as viral infections, allergic diseases and cancer. However, the success of IFN-based therapy in clinical practice is limited probably because of the short *in vivo* half-life of IFN. Therefore, IFN gene transfer has been considered to be a promising alternative to overcome this hurdle as, theoretically, it should be able to supply IFN for a long period of time (Platanias, 2005; Sadler & Williams, 2008; Bracarda et al., 2010; Kalanjeri & Sterman, 2012).

Gene therapy is defined as the transfer of a gene of interest, such as a cytokine or an antigen, into the body to treat diseases. For over two decades since the first clinical trial of gene therapy in the late 1980s (Edelstein et al., 2007), gene therapy has shown great promise in treating a variety of diseases, such as cancer, cardiovascular diseases and inherited diseases. Gene transfer can be performed using vectors, which are generally categorized as viral and non-viral. Despite their high transfection efficacy, viral vectors are generally associated with serious toxicities, high immunogenicity and a limitation in the size of the transgene incorporated into the vector. Therefore, non-viral vectors, or non-viral gene delivery systems are very attractive alternatives because of their low toxicity, low immunogenicity, and ease of preparation without any limitation of DNA loading capacity. However, the main obstacle of non-viral vectors is the low and transient transgene expression, which prevents non-viral vectors

Address for Correspondence: Yoshinobu Takakura, PhD, Department of Biopharmaceutics and Drug Metabolism, Graduate School of Pharmaceutical Sciences, Kyoto University, 46-29 Yoshidashimoadachi-cho, Sakyo-ku, Kyoto 606-8501, Japan.
E-mail: takakura@pharm.kyoto-u.ac.jp

(Received 25 June 2012; revised 21 July 2012; accepted 24 July 2012)

from exerting efficient therapeutic effects. To achieve efficient gene therapy, several advanced technologies have been developed to deliver plasmid DNA, the most frequently used non-viral vector, into target cells. This review provides an overview on current non-viral gene delivery methods, and summarizes the general ideas behind plasmid DNA modification for controlling the kinetics of transgene expression and some approaches that have been applied for IFN gene therapy in preclinical models.

Non-viral gene delivery methods

Non-viral gene delivery methods have been summarized in many review articles (Nishikawa & Huang, 2001; Nishikawa & Hashida, 2002; Mehier-Humbert & Guy, 2005; Kamimura et al., 2011). Here, we briefly show some major methods that have been used for *in vivo* gene transfer using plasmid DNA.

Non-viral methods can be divided into two main categories, physical and chemical approaches. The physical approaches cover a local or systemic injection of naked plasmid DNA by a simple needle insertion and an injection together with the application of physical or electrical forces. The latter methods generate transient pores in the plasma membrane and enhance cell membrane permeability, thus the delivery of plasmid DNA into the cytoplasm is achieved. Besides the simple injection methods, such as intramuscular injection, intratumoral injection, and so on, other well-established physical methods include hydrodynamic injection method, gene gun and electroporation. The advantages of the physical methods are the simplicity and safety.

Chemical approaches are based on the use of synthetic or natural substances that form complex with plasmid DNA through, in most cases, electrostatic interaction. Because plasmid DNA is a negatively charged polyanion, positively charged compounds, such as cationic lipids and cationic polymers, are used to obtain lipoplex or polyplex, respectively. Some methods, which combine physical and chemical methods, such as ultrasound- or magnetic field-responsive compounds, have also been invented.

Among non-viral gene delivery methods, the simple injection of naked plasmid DNA is the most popular method in clinical situations. The latest gene therapy clinical trial data indicate that the number of clinical trials using naked plasmid DNA has increased from 14% in 2004 to 18.5% in 2012 (Edelstein et al., 2004; Edelstein et al., 2007; Edelstein, 2012).

Optimization of plasmid DNA components

Two main components of plasmid DNA determine the extent of transgene expression as well as DNA production in bacteria. One is the gene control region, i.e., promoter and enhancer, which is required for regulating the transgene expression in eukaryotic cells. Another is the backbone of plasmid DNA, associated with the origin of replication and selection of marker genes, which are necessary for plasmid propagation in bacteria. The level and duration of transgene expression can be regulated by optimization of these plasmid components (Yew, 2005; van Gaal et al., 2006). Figure 1 demonstrates the schematics of the conventional plasmid and the modification of plasmid using various approaches.

Promoter/enhancer selection

The promoter is the key region for controlling the profile of transgene expression. Each promoter has a unique transgene expression profile. Therefore, selection of the optimal promoter, including other regulatory elements such as the enhancer, could control the kinetics of the transgene expression pattern of the plasmid. Various types of promoter with different expression characteristics have been reviewed (Yew, 2005). For example, CMV promoter, a widely used promoter that is derived from the regulation region of the immediate early gene of cytomegalovirus (CMV), exhibits transient expression. CMV promoter confers a strong expression of transgene but the level of transgene expression is rapidly reduced. Elongation factor 1 α (EF1α) promoter is known to exert sustained gene expression although its expression level is lower than that of CMV promoter. Therefore, optimization of the promoter and enhancer combination is an effective way of obtaining high and sustained gene expression. As a good example of promoter optimization, Magnusson et al. optimized the promoter and enhancer for high and sustained transgene expression. Switching murine CMV (mCMV) enhancer to human CMV (hCMV) enhancer resulted in the sustained expression of luciferase (Luc) activity over 80 days, whereas the Luc expression of mCMV enhancer-driven plasmid DNA fell below the limit of detection in 45 days. This sustained transgene expression achieved with hCMV enhancer might be explained by the differences in type and number of transcription factors between species. Furthermore, to combine the high level of transgene expression from CMV promoter with the sustained expression profile of EF1α promoter, the shuffle CMV-EF1α promoter (SCEP) was engineered. The expression profile from SCEP was compared with that of standard promoter, including CMV promoter and EF1α promoter with hCMV enhancer. CMV promoter showed a very transient expression profile compared with EF1α promoter and SCEP. Both EF1α promoter and SCEP showed a similar sustained expression profile. Furthermore, SCEP promoter showed a higher level of transgene expression than EF1α promoter at all time points. This study demonstrated that a sustained transgene expression can be achieved by optimizing the promoter and enhancer compartment (Magnusson et al., 2011).

Modification of plasmid DNA backbone

In addition to the promoter and enhancer, the plasmid DNA backbone should also be considered as it affects the profile of transgene expression.

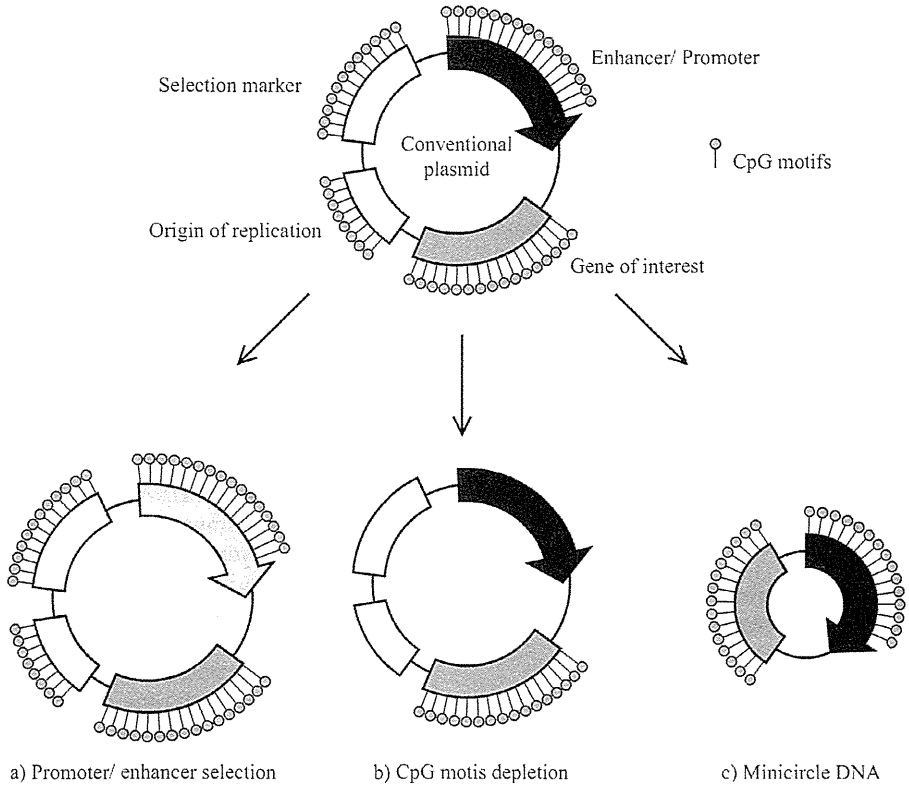

Figure 1. Schematics of conventional (unmodified) plasmid DNA (top image) and the modifications of plasmid DNA for controlling the kinetics of transgene expression: (a) promoter/enhancer selection, (b) depletion of CpG motifs from plasmid DNA and (c) elimination of plasmid bacterial backbone (minicircle DNA).

Depletion of CpG-motifs from plasmid DNA

Although plasmid DNA is less immunogenic than viral vectors, the cytosine-phosphate-guanine dinucleotides (CpG motifs) in plasmid DNA can induce inflammatory responses. The recognition of CpG motifs is mediated by Toll-like receptor 9 (TLR9), which consequently results in the generation of pro-inflammatory cytokines, such as tumor necrosis factor (TNF)-α and IFN-γ. Generally speaking, these cytokines have negative effects on transgene expression (Scheule, 2000). In addition, the methylation of cytosine residues of the CpG motifs in plasmid DNA may also be related to transgene silencing (Scheule, 2000; Takahashi et al., 2012; Yew & Cheng, 2004). Therefore, the elimination of CpG motifs from plasmid DNA could reduce immune responses to the DNA and transgene silencing, resulting in the prolongation of transgene expression. Yew et al. constructed a plasmid DNA with a reduced number of CpG motifs (Yew et al., 2002). They named this plasmid vector pGZB vector. pGZB coding chloramphenicol acetyltransferase (CAT), pGZB-sCAT (containing 102 CpG motifs), increased the duration of CAT expression in the lung and liver after *in vivo* gene transfer compared with ones consisting of conventional CpG-replete plasmid DNA (256 CpG motifs). Similar results were obtained when the CAT gene was replaced with blood coagulation factor IX. This study supported the hypothesis that persistent transgene expression is achieved by reducing the number of CpG motifs from plasmid DNA.

Minicircle DNA

Minicircle DNA, also known as a supercoiled minimal expression cassette, is an abridged form of conventional plasmid DNA obtained by eliminating all bacterial components, including a replication origin and an antibacterial resistant gene. Minicircle DNA contains only an expression cassette including cDNA, enhancer and promoter (Mayrhofer et al., 2009). The initial concept of minicircle DNA is similar to CpG reduced plasmid DNA, namely, to avoid transgene silencing mediated by bacterial-derived sequences. Several studies have reported that more persistent transgene expression is obtained with minicircle DNA compared with their parenteral plasmid DNA (Chen et al., 2003; Wu et al., 2006; Argyros et al., 2011; Huang et al., 2009), even though the mechanism whereby bacterial sequences suppress transgene expression remains unclear. Chen et al. have obtained evidence that silencing of transgene expression was not merely affected by the CpG content or CpG methylation of DNA but was mediated by the covalent linkage of the plasmid backbone to the expression cassette (Chen et al., 2004; Riu et al., 2005). They suggested that the formation of repressive heterochromatin over the plasmid DNA backbone and its ability to spread out to the adjacent

regions might be involved in the transgene silencing (Chen et al., 2004; Chen et al., 2008). Furthermore, the latest report from the same group provided strong evidence that the length but not the sequence of the DNA insert between the 5′ and 3′ ends of transgene expression cassette is critical for transgene silencing (Lu et al., 2012). Moreover, several pieces of evidence have indicated an inverse correlation between plasmid size and transgene expression efficiency (Kreiss et al., 1999; Yin et al., 2005). Considering these observations, it seems that the reduced number of CpG content is not the main factor responsible for the improved and persistent transgene expression from minicircle DNA over parenteral plasmid DNA. Instead, elimination of the plasmid bacterial backbone, shortening of the spacer between 5′ and 3′ ends of the transgene expression cassette and a reduction in plasmid size could be the reason for persistent transgene expression from minicircle DNA.

Rational design of plasmid DNA encoding the IFN gene to control the kinetics of transgene expression

The development of IFN-based therapy has been hindered by the many disadvantages of IFN, such as its short *in vivo* half-life, which requires multiple and frequent administration. These increase patient-noncompliance and the cost. Gene delivery of IFN can be used to overcome these problems. As described above, a rational design of plasmid DNA encoding the IFN gene is effective in optimizing IFN transgene expression. This section reviews the application of the strategies to IFN expressing plasmid DNA.

Improved duration of IFN transgene expression by using CpG reduced plasmid DNA

As already described, removal of CpG motifs from plasmid DNA generally results in the prolongation of transgene expression. We have demonstrated that prolonged expression of IFN-β and IFN-γ was obtained by using CpG reduced pGZB vector. A single hydrodynamic injection of pGZB vector encoding murine IFN-β (pGZB-Muβ) into mice resulted in more sustained expression of IFN-β compared with CpG-replete pCMV-Muβ. Moreover, the inhibitory effect of IFN-β gene transfer on pulmonary metastasis of CT-26 carcinoma cells was high in mice receiving pGZB-Muβ compared with that in those receiving pCMV-Muβ. Similar results were obtained with plasmids expressing murine IFN-γ. These results indicate that the removal of CpG motifs from plasmid DNA enhances the therapeutic effects of IFN gene transfer through prolongation of IFN transgene expression (Kawano et al., 2007). In order to further reduce the number of CpG motifs in plasmid DNA, CpG-free plasmid vector, called pCpG plasmid (Invivogen), which has no CpG motifs , was chosen to construct plasmid DNA encoding murine IFN-γ (pCpG-Muγ). As expected, administration of pCpG-Muγ resulted in more sustained IFN-γ expression and a greater anti-tumor effect compared with that of pGZB-Muγ or pCMV-Muγ (Mitsui et al., 2009). The sustained expression of IFN-γ from pCpG-Muγ was also beneficial in treating chronic diseases, like atopic dermatitis. We succeeded in ameliorating the development of Th2 dominant atopic dermatitis in NC/Nga mice, a mouse model of atopic dermatitis (Hattori et al., 2010). The sustained IFN-γ expression in mice shifted the immunological balance toward Th1. This effect was not observed in mice receiving multiple injections of pCMV-Muγ. Therefore, we proposed CpG depleted plasmid DNA encoding IFN-γ, pCpG-Muγ as a useful method for IFN-γ gene therapy.

Combination of CpG reduction and selection of promoter/enhancer

CpG reduced plasmid DNA encoding murine IFN-γ provided high and sustained transgene expression of IFN-γ in mice after hydrodynamic injection and produced potent therapeutic effects on tumor growth or atopic dermatitis (Mitsui et al., 2009; Hattori et al., 2010). However, the administration of pCpG-Muγ was associated with very high concentrations of IFN-γ soon after gene transfer, which fell with time to a constant, steady level. The high initial concentrations of IFNγ could induce unwanted responses, such as body weight loss. The plasmid pCpG-Muγ contains human elongation factor (hEF)-1 promoter and murine cytomegalovirus (mCMV) enhancer. The hydrodynamic injection method, which was used for gene transfer in the study of plasmid pCpG-Muγ, has been reported to activate transcription factors, including activator protein (AP)-1 and nuclear factor (NF)-kappa (κ) B in the liver (Nishikawa et al., 2008). As mCMV enhancer contains many binding sites for AP-1 and NF-κB, the activation of transcription factors by hydrodynamic injection could result in an initial surge in transgene expression. We designed and constructed a plasmid vector that exhibits a constant and steady expression of IFN-γ for minimizing the adverse effects caused by initial high concentrations of IFN-γ (Ando et al., 2012). As the kinetics of transgene expression is mainly governed by the type of promoter and enhancer, we constructed a series of plasmid vectors with different promoters and enhancers. As a result, we found that the plasmid DNA containing human ROSA26 (hROSA26) promoter produced a constant and steady expression of IFN-γ. Furthermore, adverse effects, such as body weight loss, which was observed in mice receiving a high dose pCpG-Muγ, were not observed in mice receiving hROSA promoter-driven IFNγ-expressing plasmid DNA. Lack of binding sites for AP-1 and NF-κB in the hROSA26 promoter seems to be responsible for the constant transgene expression. Interestingly, the duration of IFN-γ transgene expression from hROSA26 promoter-containing plasmid DNA was comparable with that from pCpG plasmid, despite the fact that the hROSA26 promoter contains as many as 428 CpG motifs. As the hROSA26 promoter contains many binding sites for SP1, a steady transcription

factor, sustained transgene expression from hROSA26 promoter might be due to its many SP-1 binding sites. The reason why sustained transgene expression is obtained by using the CpG replete hROSA26 promoter-driven plasmid DNA has not been identified yet. However, these results suggest that the number of CpG motifs in plasmid DNA is not a major factor controlling the profile of transgene expression.

Minicircle DNA with a tumor-selective promoter as a tumor-specific expression system

Minicircle DNA is attractive for persistent transgene expression. Wu et al. applied this DNA to IFN-γ gene therapy of cancer. The anti-tumor effects of IFN-γ on human nasopharyngeal carcinoma (NPC) were studied by using minicircle-mediated IFN-γ gene transfer. IFN-γ gene transfer by minicircle DNA exhibited better antiproliferative effects in NPC tumor-bearing mice than those obtained by its plasmid DNA counterpart, which was a consequence of a high and persistent transgene expression of IFN-γ from the minicircle DNA (Wu et al., 2006). As a close correlation between the pathogenesis of NPC and EBV infection has been reported (Raab-Traub, 2002), oriP promoter, which contains many binding sites for EBV nuclear antigen 1 (EBNA-1), was used for minicircle DNA encoding IFN-γ to increase the specificity of transgene expression in NPC tumors (Yates et al., 2000). The results obtained showed that minicircle DNA, the IFN-γ expression of which was driven by the oriP promoter, had no anti-tumor effects on EBV-negative tumor xenografts but produced tumor regression and prolonged survival in EBV positive tumor-bearing mice. Moreover, the IFN-γ level in the liver was significantly lower in mice receiving oriP promoter-based minicircle DNA than that in those receiving CMV promoter-based minicircle DNA. These findings suggest that the oriP promoter-based IFN-γ-expressing minicircle DNA can be used as a safe and effective therapy to treat EBV positive NPC (Zuo et al., 2011).

Small molecule-inducible plasmid DNA for long-term and renewable transgene expression

Drug-regulated transgene expression systems have been established to manipulate spatial and temporal aspects of transgene expression. Generally, this plasmid system consists of two key components. The first component expresses an inactive form of a regulatory protein, which will be activated after binding of a small-molecule inducer. The other one carries the transgene of interest, which is expressed in response to the activation of the regulatory protein (Nordstrom, 2003). A mifepristone (MFP)-inducible plasmid system, termed pBRES has been constructed by Szymanski et al. A variety of transgenes, including human IFNβ, were inserted into the pBRES plasmid and the regulation of transgene expression in response to MFP was examined. For example, the intraperitoneal injection of MFP following the transfection of pBRES plasmid encoding human IFNβ (pBRES-hIFNβ) into murine hind limb muscles with electroporation resulted in detectable serum levels of hIFNβ while, in the absence of MFP, the level of hIFNβ in mouse serum was undetectable (Szymanski et al., 2007). Harkins et al. applied the pBRES plasmid system for encoding murine IFN-β and investigated the therapeutic effect in a murine model of experimental allergic encephalomyelitis (EAE). This plasmid DNA induced efficient and sustained expression of interferon-inducible protein-10, which is used as a marker of IFN activity, in mice for up to 3 months under MFP induction. Repeated administration of plasmid resulted in renewed expression. The administration of the pBRES murine IFNβ plasmid with an inducer MFP produced an efficient therapeutic effect compared with the control plasmid or pBRES murine IFN-β plasmid administration without MFP in a mouse model of EAE (Harkins et al., 2008).

Conclusions

IFN gene transfer could avoid the many drawbacks of IFN-based therapy and a number of clinical trials have been conducted using IFN gene transfer (Kalanjeri & Sterman, 2012). However, most of these studies use viral vectors. Only few studies were conducted using non-viral vectors like cationic liposomes (Matsumoto et al., 2008; Wakabayashi et al., 2008). In order to expand the range of IFN gene therapy by plasmid DNA vector, an engineered plasmid DNA vector that can regulate spatio-temporal distribution of IFN is required. In the present review, we have summarized attractive strategies that can be used to obtain more precisely controlled transgene expression of IFN from modified plasmid DNA, which could be applied via simple administration methods, such as hydrodynamic injection (Ando et al., 2012; Hattori et al., 2010; Mitsui et al., 2009), intramuscular injection (Harkins et al., 2008), and intratumoral injection of plasmid DNA/cationic liposome complex (Wu et al., 2006; Zuo et al., 2011). Using plasmid modification techniques described in the present review is a promising strategy for improving the therapeutic efficacy and safety profile of IFN gene therapy.

Declaration of interest

The authors report no conflicts of interest.

References

Ando M, Takahashi Y, Nishikawa M, Watanabe Y, Takakura Y. (2012). Constant and steady transgene expression of interferon-γ by optimization of plasmid construct for safe and effective interferon-γ gene therapy. J Gene Med, 14, 288–295.

Argyros O, Wong SP, Fedonidis C, Tolmachov O, Waddington SN, Howe SJ, Niceta M, Coutelle C, Harbottle RP. (2011). Development of S/MAR minicircles for enhanced and persistent transgene expression in the mouse liver. J Mol Med, 89, 515–529.

Bracarda S, Eggermont AM, Samuelsson J. (2010). Redefining the role of interferon in the treatment of malignant diseases. Eur J Cancer, 46, 284–297.

Chen ZY, He CY, Ehrhardt A, Kay MA. (2003). Minicircle DNA vectors devoid of bacterial DNA result in persistent and high-level transgene expression in vivo. Mol Ther, 8, 495–500.

Chen ZY, He CY, Meuse L, Kay MA. (2004). Silencing of episomal transgene expression by plasmid bacterial DNA elements in vivo. Gene Ther, 11, 856–864.

Chen ZY, Riu E, He CY, Xu H, Kay MA. (2008). Silencing of episomal transgene expression in liver by plasmid bacterial backbone DNA is independent of CpG methylation. Mol Ther, 16, 548–556.

Edelstein M. (2012). Gene therapy clinical trials worldwide [Online]. John Wiley and Sons Ltd. Available: http://www.wiley.com/legacy/wileychi/genmed/clinical/ [Accessed 24 April 2012].

Edelstein ML, Abedi MR, Wixon J. (2007). Gene therapy clinical trials worldwide to 2007–an update. J Gene Med, 9, 833–842.

Edelstein ML, Abedi MR, Wixon J, Edelstein RM. (2004). Gene therapy clinical trials worldwide 1989-2004-an overview. J Gene Med, 6, 597–602.

Harkins RN, Szymanski P, Petry H, Brooks A, Qian HS, Schaefer C, Kretschmer PJ, Orme A, Wang P, Rubanyi GM, Hermiston TW. (2008). Regulated expression of the interferon-beta gene in mice. Gene Ther, 15, 1–11.

Hattori K, Nishikawa M, Watcharanurak K, Ikoma A, Kabashima K, Toyota H, Takahashi Y, Takahashi R, Watanabe Y, Takakura Y. (2010). Sustained exogenous expression of therapeutic levels of IFN-gamma ameliorates atopic dermatitis in NC/Nga mice via Th1 polarization. J Immunol, 184, 2729–2735.

Huang M, Chen Z, Hu S, Jia F, Li Z, Hoyt G, Robbins RC, Kay MA, Wu JC. (2009). Novel minicircle vector for gene therapy in murine myocardial infarction. Circulation, 120, S230–S237.

Kalanjeri S, Sterman D. (2012). Gene therapy in interventional pulmonology: Interferon gene delivery with focus on thoracic malignancies. Curr Resp Care Rep, 1, 54–66.

Kamimura K, Suda T, Zhang G, Liu D. (2011). Advances in Gene Delivery Systems. Pharmaceut Med, 25, 293–306.

Kawano H, Nishikawa M, Mitsui M, Takahashi Y, Kako K, Yamaoka K, Watanabe Y, Takakura Y. (2007). Improved anti-cancer effect of interferon gene transfer by sustained expression using CpG-reduced plasmid DNA. Int J Cancer, 121, 401–406.

Kreiss P, Cameron B, Rangara R, Mailhe P, Aguerre-Charriol O, Airiau M, Scherman D, Crouzet J, Pitard B. (1999). Plasmid DNA size does not affect the physicochemical properties of lipoplexes but modulates gene transfer efficiency. Nucleic Acids Res, 27, 3792–3798.

Lu J, Zhang F, Xu S, Fire AZ, Kay MA. (2012). The extragenic spacer length between the 5' and 3' ends of the transgene expression cassette affects transgene silencing from plasmid-based vectors. Mol Ther. DOI: 10.1038/mt.2012.65.

Magnusson T, Haase R, Schleef M, Wagner E, Ogris M. (2011). Sustained, high transgene expression in liver with plasmid vectors using optimized promoter-enhancer combinations. J Gene Med, 13, 382–391.

Matsumoto K, Kubo H, Murata H, Uhara H, Takata M, Shibata S, Yasue S, Sakakibara A, Tomita Y, Kageshita T, Kawakami Y, Mizuno M, Yoshida J, Saida T. (2008). A pilot study of human interferon beta gene therapy for patients with advanced melanoma by *in vivo* transduction using cationic liposomes. Jpn J Clin Oncol, 38, 849–856.

Mayrhofer P, Schleef M, Jechlinger W. (2009). Use of minicircle plasmids for gene therapy. Methods Mol Biol, 542, 87–104.

Mehier-Humbert S, Guy RH. (2005). Physical methods for gene transfer: improving the kinetics of gene delivery into cells. Adv Drug Deliv Rev, 57, 733–753.

Mitsui M, Nishikawa M, Zang L, Ando M, Hattori K, Takahashi Y, Watanabe Y, Takakura Y. (2009). Effect of the content of unmethylated CpG dinucleotides in plasmid DNA on the sustainability of transgene expression. J Gene Med, 11, 435–443.

Nishikawa M, Hashida M. (2002). Nonviral approaches satisfying various requirements for effective *in vivo* gene therapy. Biol Pharm Bull, 25, 275–283.

Nishikawa M, Huang L. (2001). Nonviral vectors in the new millennium: delivery barriers in gene transfer. Hum Gene Ther, 12, 861–870.

Nishikawa M, Nakayama A, Takahashi Y, Fukuhara Y, Takakura Y. (2008). Reactivation of silenced transgene expression in mouse liver by rapid, large-volume injection of isotonic solution. Hum Gene Ther, 19, 1009–1020.

Nordstrom JL. (2003). The antiprogestin-dependent GeneSwitch system for regulated gene therapy. Steroids, 68, 1085–1094.

Platanias LC. (2005). Mechanisms of type-I- and type-II-interferon-mediated signalling. Nat Rev Immunol, 5, 375–386.

Raab-Traub N. (2002). Epstein-Barr virus in the pathogenesis of NPC. Semin Cancer Biol, 12, 431–441.

Riu E, Grimm D, Huang Z, Kay MA. (2005). Increased maintenance and persistence of transgenes by excision of expression cassettes from plasmid sequences in vivo. Hum Gene Ther, 16, 558–570.

Sadler AJ, Williams BR. (2008). Interferon-inducible antiviral effectors. Nat Rev Immunol, 8, 559–568.

Scheule RK. (2000). The role of CpG motifs in immunostimulation and gene therapy. Adv Drug Deliv Rev, 44, 119–134.

Szymanski P, Kretschmer PJ, Bauzon M, Jin F, Qian HS, Rubanyi GM, Harkins RN, Hermiston TW. (2007). Development and validation of a robust and versatile one-plasmid regulated gene expression system. Mol Ther, 15, 1340–1347.

Takahashi Y, Nishikawa M, Takakura Y. (2012). Development of safe and effective nonviral gene therapy by eliminating CpG motifs from plasmid DNA vector. Front Biosci (Schol Ed), 4, 133–141.

van Gaal EV, Hennink WE, Crommelin DJ, Mastrobattista E. (2006). Plasmid engineering for controlled and sustained gene expression for nonviral gene therapy. Pharm Res, 23, 1053–1074.

Wakabayashi T, Natsume A, Hashizume Y, Fujii M, Mizuno M, Yoshida J. (2008). A phase I clinical trial of interferon-beta gene therapy for high-grade glioma: novel findings from gene expression profiling and autopsy. J Gene Med, 10, 329–339.

Wu J, Xiao X, Zhao P, Xue G, Zhu Y, Zhu X, Zheng L, Zeng Y, Huang W. (2006). Minicircle-IFNgamma induces antiproliferative and antitumoral effects in human nasopharyngeal carcinoma. Clin Cancer Res, 12, 4702–4713.

Yates JL, Camiolo SM, Bashaw JM. (2000). The minimal replicator of Epstein-Barr virus oriP. J Virol, 74, 4512–4522.

Yew NS. (2005). Controlling the kinetics of transgene expression by plasmid design. Adv Drug Deliv Rev, 57, 769–780.

Yew NS, Cheng SH. (2004). Reducing the immunostimulatory activity of CpG-containing plasmid DNA vectors for non-viral gene therapy. Expert Opin Drug Deliv, 1, 115–125.

Yew NS, Zhao H, Przybylska M, Wu IH, Tousignant JD, Scheule RK, Cheng SH. (2002). CpG-depleted plasmid DNA vectors with enhanced safety and long-term gene expression in vivo. Mol Ther, 5, 731–738.

Yin W, Xiang P, Li Q. (2005). Investigations of the effect of DNA size in transient transfection assay using dual luciferase system. Anal Biochem, 346, 289–294.

Zuo Y, Wu J, Xu Z, Yang S, Yan H, Tan L, Meng X, Ying X, Liu R, Kang T, Huang W. (2011). Minicircle-oriP-IFNγ: a novel targeted gene therapeutic system for EBV positive human nasopharyngeal carcinoma. PLoS ONE, 6, e19407.